GEOSPHERE

GEOSPHERE, v. 17, no. 5

https://doi.org/10.1130/GES02264.1

11 figures; 1 table; 1 set of supplemental files

CORRESPONDENCE: jejembi@siu.edu

CITATION: Ejembi, J.I., Potter-McIntyre, S.L., Sharman, G.R., Smith, T.M., Saylor, J.E., Hatfield, K., and Ferré, E.C., 2021, Detrital zircon geochronology and provenance of the Middle to Late Jurassic Paradox Basin and Central Colorado trough: Paleogeographic implications for southwestern Laurentia: Geosphere, v. 17, no. 5, p. 1494-1516, https://doi.org/10.1130 /GES02264.1.

Science Editor: David E. Fastovsky Associate Editor: Graham D.M. Andrews

Received 1 April 2020 Revision received 20 January 2021 Accepted 22 April 2021

Published online 21 July 2021





This paper is published under the terms of the CC-BY-NC license

© 2021 The Authors

Detrital zircon geochronology and provenance of the Middle to Late Jurassic Paradox Basin and Central Colorado trough: **Paleogeographic implications for southwestern Laurentia**

John I. Ejembi¹, Sally L. Potter-McIntyre¹, Glenn R. Sharman², Tyson M. Smith³, Joel E. Saylor³*, Kendall Hatfield³, and Eric C. Ferré⁴

- ¹Department of Geology, Southern Illinois University, Carbondale, Illinois 62901, USA
- ²Department of Geosciences, University of Arkansas, Fayetteville, Arkansas 72701, USA
- ³Department of Earth and Atmospheric Sciences, University of Houston, Houston, Texas 77207, USA
- ⁴School of Geosciences, University of Louisiana at Lafayette, Lafayette, Louisiana 70504, USA

ABSTRACT

Middle to Upper Jurassic strata in the Paradox Basin and Central Colorado trough (CCT; southwestern United States) record a pronounced change in sediment dispersal from dominantly aeolian deposition with an Appalachian source (Entrada Sandstone) to dominantly fluvial deposition with a source in the Mogollon and/or Sevier orogenic highlands (Salt Wash Member of the Morrison Formation). An enigmatic abundance of Cambrian (ca. 527-519 Ma) grains at this provenance transition in the CCT at Escalante Canyon, Colorado, was recently suggested to reflect a local sediment source from the Ancestral Front Range, despite previous interpretations that local basement uplifts were largely buried by Middle to Late Jurassic time.

This study aims to delineate spatial and temporal patterns in provenance of these Jurassic sandstones containing Cambrian grains within the Paradox Basin and CCT using sandstone petrography, detrital zircon U-Pb geochronology, and detrital zircon trace elemental and rare-earth elemental (REE) geochemistry. We report 7887 new U-Pb detrital zircon analyses from 31 sandstone samples collected within seven transects in western Colorado and eastern Utah. Three clusters of

John Ejembi https://orcid.org/0000-0002-4562-7427 *Now at the Department of Earth, Ocean and Atmospheric Sci-

ences, University of British Columbia, Vancouver, British Columbia V6T 1Z4, Canada

zircon ages are consistently present (1.53-1.3 Ga, 1.3-0.9 Ga, and 500-300 Ma) that are interpreted to reflect sources associated with the Appalachian orogen in southeastern Laurentia (mid-continent, Grenville, Appalachian, and peri-Gondwanan terranes). Ca. 540-500 Ma zircon grains are anomalously abundant locally in the uppermost Entrada Sandstone and Wanakah Formation but are either lacking or present in small fractions in the overlying Salt Wash and Tidwell Members of the Morrison Formation. A comparison of zircon REE geochemistry between Cambrian detrital zircon and igneous zircon from potential sources shows that these 540-500 Ma detrital zircon are primarily magmatic. Although variability in both detrital and igneous REE concentrations precludes definitive identification of provenance, several considerations suggest that distal sources from the Cambrian granitic and rhyolitic provinces of the Southern Oklahoma aulacogen is also likely, in addition to a proximal source identified in the McClure Mountain syenite of the Wet Mountains, Colorado. The abundance of Cambrian grains in samples from the central CCT, particularly in the Entrada Sandstone and Wanakah Formation, suggests northwesterly sediment transport within the CCT, with sediment sourced from Ancestral Rocky Mountains uplifts of the southern Wet Mountains and/or Amarillo-Wichita Mountains in southwestern Oklahoma. The lack of Cambrian grains within the Paradox Basin suggests that the Uncompangre uplift (southwestern Colorado) acted as a barrier to sediment transport from the CCT.

INTRODUCTION

The Colorado Plateau in the southwestern United States preserves a nearly continuous record of Jurassic continental and marginal marine deposition that has been widely studied as an archive of the tectonic, climatic, and biotic evolution of western Laurentia (Kocurek and Dott, 1983; Blakey, 1994; DeCelles, 2004; Foster and Lucas, 2006). To place the Jurassic stratigraphy of the Colorado Plateau within a paleogeographic context, previous workers used sediment provenance to infer patterns of sediment dispersal via fluvial, aeolian, and marine processes (Kocurek and Dott, 1983; Peterson, 1988, 1994; Blakey, 1994). In the 2000s, a number of studies made significant advancements in refining understanding of sediment sources and transport pathways to the Mesozoic Colorado Plateau, largely due to the improved provenance resolution afforded by detrital zircon U-Pb geochronology via laser ablation (Rahl et al., 2003; Dickinson and Gehrels, 2003, 2008a, 2008b, 2009, 2010). As summarized by Dickinson and Gehrels (2010), three dominant middle Mesozoic sediment routing patterns were recognized on the basis of detrital zircon U-Pb ages and other geologic information: (1) northwesterly sediment transport from the Marathon-Quachita orogen and rift flank of the Gulf of Mexico during deposition of the Upper Triassic Chinle Formation, (2) transcontinental sediment transport from the distant Appalachian orogen westward across the craton and subsequent reworking into Lower to Middle Jurassic sand sheets, and (3) northerly

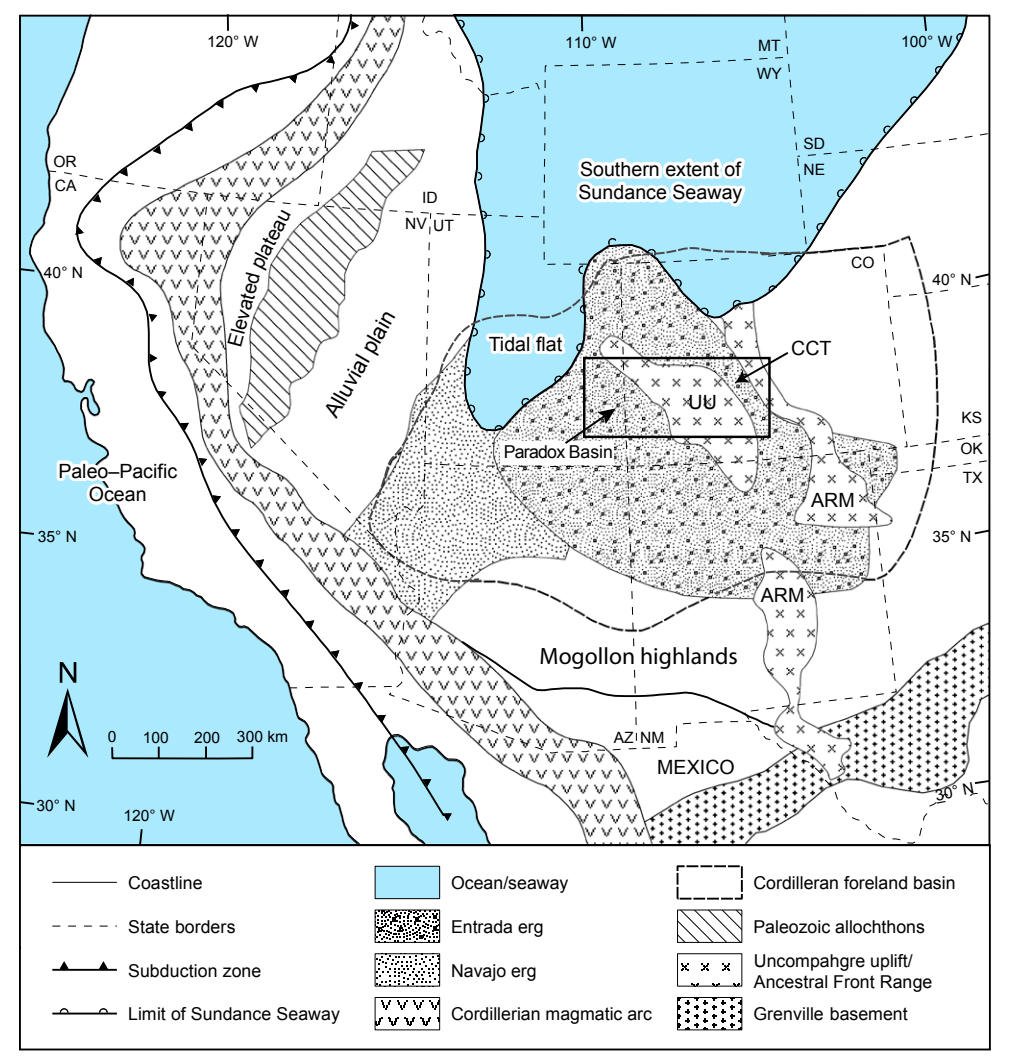


Figure 1. Major tectonic elements and deposystems of the western United States during the Jurassic (after Lawton, 1994; Barbeau, 2003; Dickinson and Gehrels, 2003, 2008a; Blakey, 2012). UU—Uncompahgre uplift; ARM—Ancestral Rocky Mountains; CCT—Central Colorado trough. Black box is the outline of the study area map shown in Figure 3. Solid black line beneath the Mogollon highlands is its southern limit. State abbreviations: OR—Oregon; CA—California; ID—Idaho; NV—Nevada; UT—Utah; AZ—Arizona; MT—Montana; WY—Wyoming; CO—Colorado; NM—New Mexico; SD—South Dakota; NE—Nebraska; KS—Kansas; OK—Oklahoma; TX—Texas.

and northeasterly sediment transport from the Mogollon and Sevier orogenic highlands during deposition of Upper Jurassic and Cretaceous units of the Western Interior Basin.

Although many middle Mesozoic units of the Colorado Plateau share a similar detrital zircon U-Pb age signature that reflects an ultimate origin from the Appalachian orogen and/or associated sedimentary basins (Dickinson and Gehrels, 2010), Dickinson and Gehrels (2008b) identified three samples from the Upper Triassic Chinle-Dockum (Dickinson et al., 2010 and Dickinson and Gehrels, 2008) fluvial sandstones that had anomalous abundances of Cambrian zircon, an age group that had not been found, at that time, in unusual abundances in younger (Jurassic-Cretaceous) strata (Dickinson and Gehrels, 2009). Potter-McIntyre et al. (2016) identified high abundances of Cambrian grains in the Middle and Upper Jurassic units within the Central Colorado trough (CCT) with similar age peaks (519-527 Ma) as in the underlying Chinle Formation (515-523 Ma; Dickinson and Gehrels, 2008b) (Fig. 1). While Dickinson and Gehrels (2008b) interpreted a sediment source from the Southern Oklahoma aulacogen for these Cambrian grains, Potter-McIntyre et al. (2016) inferred a local source from the Wet Mountains of southern Colorado (ca. 523 Ma McClure Mountain syenite; Schoene and Bowring, 2006), implying that the Ancestral Front Range remained a locally important sediment source well into Late Jurassic time, later than previously thought (Dickinson and Gehrels, 2003). Unlike many other orogenic belts that are distributed across wide regions of Laurentia (e.g., Grenville and Appalachian belts; Whitmeyer and Karlstrom, 2007), Cambrian protosources (sensu Pell et al., 1997) are primarily restricted to a few geographically restricted locations within the western United States, including central Colorado and Oklahoma (Powell et al., 1980; Larson et al., 1985; Hogan and Gilbert, 1998; Schoene and Bowring, 2006; Hanson et al., 2009). Thus, identification of the source of Cambrian detrital zircon, where present, may allow a greater degree of provenance specificity than is usually afforded with detrital zircon studies of central Laurentia.

The geologic significance of the spatial and temporal extent of Cambrian grains within

Middle-Upper Jurassic units of the central Colorado Plateau and adjacent Paradox Basin is uncertain because results of Potter-McIntyre et al. (2016) included samples from only a single section at Escalante Canyon, Colorado. This study aims to delineate the geographic and temporal distribution of this distinctive Cambrian age group within Middle-Upper Jurassic units of the CCT of western Colorado and eastern Utah. The units included in this study span the transition between aeolian units of Appalachian provenance (Entrada Sandstone; Dickinson and Gehrels, 2003) and fluvial units of Mogollon and Sevier provenance (Morrison Formation; Dickinson and Gehrels, 2008a) that have contrasting dominant sediment transport vectors (i.e., aeolian units sourced from the north-northeast and fluvial units sourced from the west-southwest) We used a multiproxy approach to provenance analysis, including incorporation of bulk sandstone mineralogy (modal point counts of framework grains from 12 samples), detrital zircon U-Pb geochronology (7887 new analyses from 31 sandstone samples), and detrital zircon trace and rare-earth elemental (REE) geochemistry (111 analyses of Cambrian detrital zircon from seven samples, and 163 analyses of Cambrian igneous zircon from five samples). This study includes seven additional transects in addition to the original section and detrital zircon U-Pb ages reported by Potter-McIntyre et al. (2016) from Escalante Canyon (693 analyses from seven samples). Numerical sediment unmixing using non-negative matrix factorization (Sharman and Johnstone, 2017; Saylor et al., 2019) on the combined data set (this study and data from Potter-McIntyre et al. [2016]) provides a quantitative estimate of the contributions of the Cambrian and other sources of detrital zircon across the Middle to Late Jurassic time in the Paradox Basin and CCT. This study clarifies patterns of sediment routing during the Middle-Late Jurassic transition and suggests the existence of a northwesterly sediment dispersal system that transported detritus from the relict Ancestral Rocky Mountains uplifts within south-central Colorado and possibly as far as Oklahoma into the CCT, similar to the Eagle paleorive of the older, Chinle-Dockum depositional system (Dickinson and Gehrels, 2008b).

■ GEOLOGIC BACKGROUND

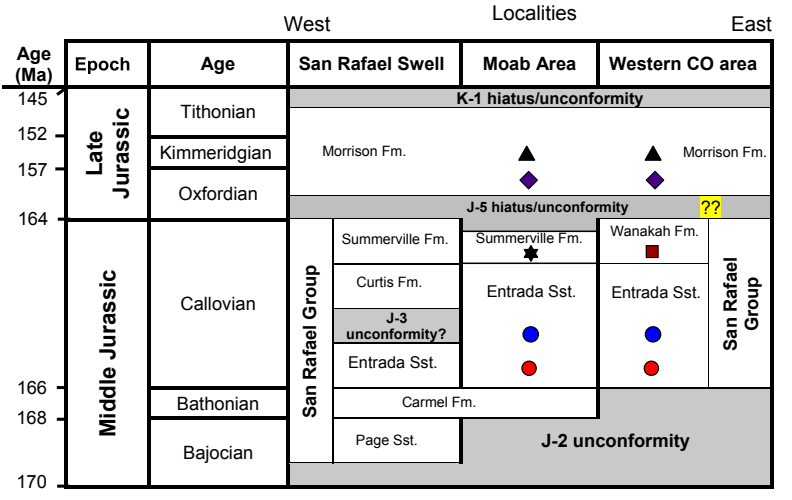
The Paradox Basin and CCT formed in response to crustal loading and downward flexure along the margins of the Uncompangre uplift and Ancestral Front Range during the Pennsylvanian-Permian Ancestral Rocky Mountains (ARM) orogeny in Utah and Colorado (Fig. 1; e.g., Kluth and Coney, 1981; Hoy and Ridgway, 2002; Barbeau, 2003). The ARM orogeny manifested as the deformation of the Cordilleran foreland basin and intracratonic block uplifts that occurred during the collision and suturing of the North and South American plates along the Appalachian-Ouachita-Marathon thrust belt (Barbeau, 2003). In central Colorado, the Ancestral Front Range, part of the ARM orogeny that consisted of the Front Range uplift, Wet Mountains, and Sangre de Cristo Mountains, formed the northwest-trending eastern boundary of the CCT (Hoy and Ridgway, 2002; Fig. 1). The northwest-southeast-trending Uncompangre uplift borders the CCT to the west and separates the Paradox Basin from the CCT. Following the ARM orogeny, magmatism occurred during Middle to Late Jurassic time along western North America (Fig. 1) in response to either subduction of the oceanic plates beneath the North American continent (e.g., Lawton, 1994; DeCelles, 2004) or collision of accreted terranes against the western continental margin (e.g., Colpron et al., 2015). Along the southern continental margin, a combination of Late Jurassic rifting and magmatism created the Mogollon highlands south of the Paradox Basin (Fig. 1; Dickinson and Lawton, 2001). Several foreland basins—commonly referred to as the ARM basins—formed adjacent to the ARM uplifts (Barbeau, 2003) and were sites for sedimentation during the Mesozoic.

In Early Jurassic time, fluvial and aeolian sediments derived from the magmatic arc and sources in southeastern Laurentia accumulated as the Glen Canyon Group in a broad retroarc foreland that developed on the Colorado Plateau, east of the western Cordillera (Peterson, 1994; Dickinson and Gehrels, 2009). The J-2 unconformity (Fig. 2), an erosional unconformity that separates the Middle Jurassic San Rafael Group from the older Glen Canyon Group, resulted from the eastward migration

of the magmatic arc and forebulge toward the continental interior in response to the flattening of the subducting oceanic plate (Pipiringos and O'Sullivan, 1978; Lawton, 1994). The San Rafael Group (Fig. 2) is widespread and is well exposed in western Colorado and Utah.

By Middle Jurassic time, the regional climate in western Laurentia had shifted from arid to temperate conditions (Busby et al., 2005), with intermittent marine transgressions from the north into the continent interior reworking aeolian sediments into fluvio-deltaic deposits on the southern margin of the impinging seaway (Fig. 1; Pipiringos and O'Sullivan, 1978; Blakey, 1994). The regression of the seaway may have created several freshwater lakes (Tanner, 1970) in western intracratonic basins, which later evolved into hypersaline lakes. One of these hypersaline lakes formed in the Paradox Basin and CCT during Middle Jurassic time (ca. 165 Ma), wherein the Wanakah Formation and the Tidwell Member of the Morrison Formation were deposited (Blakey and Ranney, 2008; Potter-McIntyre et al., 2016).

Potter-McIntyre et al. (2016) attributed the origin of the lake system in the Paradox Basin and CCT to stream capture and drainage reorganization, with a major drainage channel directed from the Ancestral Front Range in central Colorado. Hypothetically, the Paradox Basin and CCT may also have drained the north-facing Mogollon slope, the southeastern Ancestral Rockies, and the Appalachian highlands during Middle-Late Jurassic time (Fig. 1). Pulses in sedimentation during Middle-Late Jurassic time on the Colorado Plateau are marked by regional unconformities (Fig. 2). These unconformities are mostly erosional surfaces and are hypothesized to have occurred due to tilting of the Colorado Plateau and/or major sea-level regression (Peterson, 1994; O'Sullivan, 2004). The J-5 unconformity is placed underneath the basal sandstone (marker bed A) of the Tidwell Member of the Morrison Formation and is interpreted to extend throughout western Colorado and westward into the San Rafael Swell in Utah (Fig. 2). The J-5 unconformity has also been interpreted across Laurentia as co-occurring with a major sea-level regression and represents a relatively short time span (~2 m.y.; Peterson, 1994).



Units sampled

- ▲ Salt Wash Mbr.
- Tidwell Mbr.Wanakah Fm.
- Summerville Fm.
- Entrada Sst.Board beds

ition of unconformities

Figure 2. Stratigraphic nomenclature of Middle and Upper Jurassic units with the relative position of unconformities in the San Rafael Swell and Moab area (Utah) and western Colorado (CO), USA (after O'Sullivan, 1992, 2004, 2010). Colored shapes denote sampled units. Sampling sites for this study (two in the Moab area and five in the western Colorado area) are shown in Figure 3. See Pipringos and O'Sullivan (1978) for details on the unconformities. Highlighted question marks in the Western CO Area column indicate the J-5 unconformity is not widely accepted within the community to extend into western Colorado. See discussion in the manuscript text. Fm. — Formation; Sst. — Sandstone; Mbr. — Member.

The occurrence, lateral extent, and stratigraphic placement of the J-5 unconformity in western Laurentia have been a subject of debate (Fig. 2; Carr-Crabaugh and Kocurek, 1998; O'Sullivan, 2004; Dickinson and Gehrels, 2008a; Potter-McIntyre et al., 2016). The Wanakah Formation and its coeval lateral equivalent, the Summerville Formation, lie stratigraphically between the Middle Jurassic Entrada Sandstone and the Tidwell Member of the Upper Jurassic Morrison Formation in western Colorado and southeastern Utah, respectively (Fig. 2; O'Sullivan, 1980; 1992; Scott et al., 2001).

Late Jurassic (ca. 160 Ma) deposition occurred in an extensive alluvial plain, with the depositional environment shifting from lacustrine (Tidwell Member) to fluvial and fluvio-lacustrine (Salt Wash and Brushy Basin Members), coincident with two episodes of marine transgressions in Oxfordian and Kimmeridgian time (Peterson, 1994; Demko et al., 2004; Bernier and Chan, 2006). Paleocurrent data indicate that sediments deposited in Western Interior Basins during Late Jurassic time came from

the magmatic arcs to the west and from southern Laurentia (Lawton, 1994; DeCelles, 2004).

METHODS

Field and Sampling Methods

We measured stratigraphic sections and collected rock samples from seven new localities along a northwest-southeast transect across central Colorado and southeastern Utah (Fig. 3). We collected sandstone samples from the following units in localities where they are present and/or exposed: (1) the Entrada Sandstone, (2) the "board beds" of the Entrada Sandstone (informally named set of uppermost sandstone beds known for its distinctive stack of unevenly weathering beds; e.g., O'Sullivan, 2004), (3) the Wanakah Formation, (4) the Summerville Formation, (5) the Tidwell Member of the Morrison Formation, and (6) the Salt Wash Member of the Morrison Formation. We collected

an average of two samples from each 4 m interval from each sandstone unit (usually at the base, middle, and top) and/or at intervals where distinct changes in lithology occur. We used the methods of Powers (1953) and Jerram (2001) to characterize sandstone texture and the Dickinson and Suczek (1979) method to analyze the petrographic abundance of framework grains in all samples (Fig. 4).

Sample Preparation and Analytical Methods

Zircon grains were separated from pulverized sandstone samples (each 10-15 kg) using standard techniques of hydraulic, density, and magnetic separation. The U-Pb ages of detrital zircon grains were determined using laser ablation-inductively coupled plasma mass spectrometry (LA-ICPMS) at the University of Arizona LaserChron Laboratory (Tucson, Arizona, USA) following well-established methods (Gehrels et al., 2006, 2008; Gehrels, 2012). We used backscatter images to characterize the shape of the zircon grains and as a guide for selecting target spots for laser ablation and analyses. Zircon grains were selected randomly (i.e., regardless of the degree of rounding, grain size, shape, or color), except that zircon grains with fractured surfaces or those that appeared to have damaged cores were not targeted to avoid acquiring unreliable ages that could result from Pb loss, secondary inclusions of minerals, or surface irregularities (Gehrels, 2012).

We corrected the U-Pb age of both standards and unknown zircon grains using E2AgeCalc, a Python decoding routine and raw data reduction program available at the LaserChron Laboratory. Zircon grains with concordant ages were retained and used for provenance analyses. By comparing the $^{206}\text{Pb}/^{238}\text{U}$ age for <1000 Ma grains and $^{206}\text{Pb}/^{207}\text{Pb}$ age for >1000 Ma grains, we set a maximum discordance filter to >30% discordant and <5% reverse discordant for all $^{206}\text{Pb}/^{238}\text{U}$ analyses >400 Ma. In total, we retained 7887 analyses from our data set, ~94% of the total number. Age uncertainties are reported at a 2σ confidence level (~1%–2% relative uncertainty). The U-Pb ages of zircon grains per sample are plotted as kernel density estimates

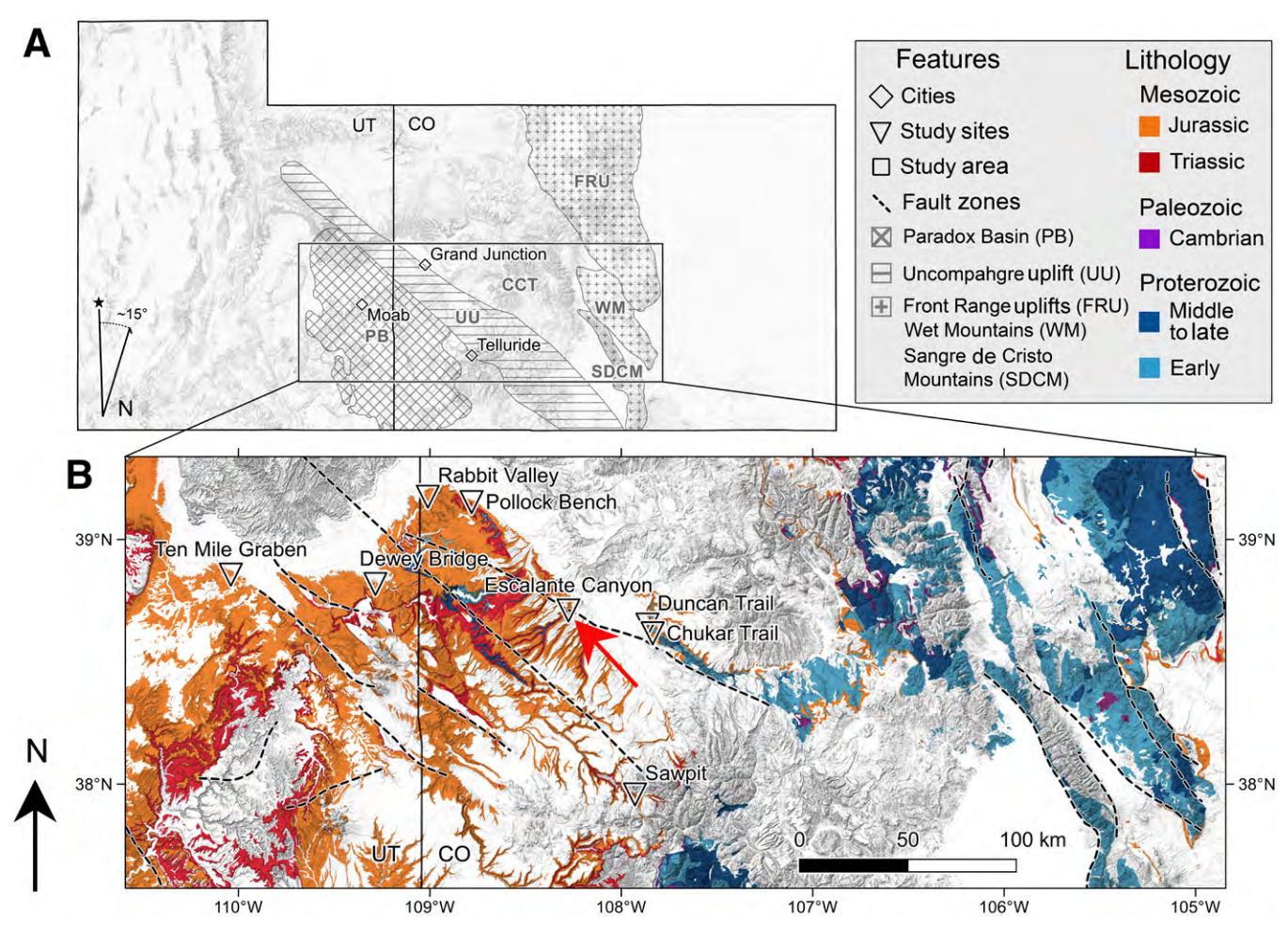


Figure 3. Geologic map of the study area in the western United States (Cashion, 1973; Steven et al., 1974; Tweto et al., 1976, 1978). (A) Outline of the Paradox Basin and locations of tectonic elements in Utah (UT) and Colorado (CO). (B) Area of rectangular box in A showing the distribution of Jurassic and Triassic sedimentary rocks in the Paradox Basin in western Colorado and southeastern Utah and basement rocks (mostly igneous intrusives) of the southern Ancestral Front Range. Early Proterozoic rocks are 1.8–1.6 Ga schists and gneisses, and 1.7 Ga granitic rocks; middle–late Proterozoic rocks are 1.4 Ga granitic rocks and 1.1 Ga graniticis of the Pikes Peak batholith. Red arrow points to the intersection of the east-west and southeast-northwest transects of the sampling sites within the Paradox Basin and Central Colorado trough (CCT), which cover ~19,000 km². Background image is from the USGS shaded relief and digital elevation model maps of the area available at https://apps.nationalmap.gov/downloader/#/, https://ngmdb.usgs.gov/topoview/viewer/#9/39.4627/-107.8349.

Table St	Major	peaks of age	clusters of d	etritali zircon	and their oral	n percentages i	the Middle-U	oer Jurassic st	rata, Parados 9	lasin, western	United State
-						accomen to					
Marine Marine	200	12756	20.00	100.000	171 - NOW	22-2290	0.00 - 1.00 mg	155,1836	78000000000000000000000000000000000000	111,7750	2742 192
Contract of	4.0	,	,	,		J	,,,,,,,,,,,,,,,,,,,,,,,,,,,,,,,,,,,,,,,	,,,,,,,,,,,,,,,,,,,,,,,,,,,,,,,,,,,,,,,	31	,,,,,,,,,,,,,,,,,,,,,,,,,,,,,,,,,,,,,,,	,,,,,,,,,,,,,,,,,,,,,,,,,,,,,,,,,,,,,,,
		0.475	FOR SHIP	0.12	15 4 50 60	200 M THE TAIR	100 10 1000	15 (1.77)		0.000	0.155
Arr	-	27.77	10.4 10.10		White the same	FOLK 100 110	100.0 100.100	10 × 100	D. P. TO. 100	to present our	0155
	-	5.440									
-	- 3		PER SECTION	D L SE	TO DE STATE OF	MALE THE THE	10.0 100	NAME AND ADDRESS OF THE PARTY AND ADDRESS OF T	0.000		0.170
140	-		100-14-181	10 p 60;	P-1-22	MALE WALLES	THE P WISE	95 p 1800	20 H 1885		
-											
100	- 12	DATE:	100.000	DATE	Put TO	200 H THE TOTAL	D-12 (00)	District Str.	D 10 700	ALMER	DATE
	-										
		27.5	20,000	Direction .	0.475	PER MANAGEMENT	10.4 100	20110	2177		D. J. CO.
144	-	PLU THAN	No work	ALC: NO	With Miles	ALT IN THE LINE	THE PLANS	THE PERSON	PLATER THE	This series	A PART
Anna ber											
- 64	40.	NAME OF	275 p. 200, 271	-	170,000,000	200 p. mil. 1 mj.	100-31 (100-100)	Ph. J. Sec. 141.	59.90	A y and	A-3-88
NAME OF	-	Division.	100 (100 (10)		D. J. St.	100 to 100 Test	Page 100	10.0 00.00	2122	0.000	NAME OF
MW	100	Auman	FO 4 10 400		The print and	FO 2 THE THE	100-y 100-100	THE RES LESS	2122	0.100	0.150
146	-	A Print	100 (4.80,48)	The party	P-1-mil	May be prove a until	Physical Property	THE RESERVED.	wh mil	O-press	Open.
Automatic to	900,000										
18	- 8	105 p. 107 (10)	15 (15 (15)	-	15 (150.00)	MS (4.100, 140)	Web 200, 185	ALC: 100, 100,	_	-	_
200	- 2	P. U. Mil.	Children and		Philip tea next	100 pt 100 T (0)	TO 2 THE LAST	Die ter tan	D. P. 180		
100	-			BA 2 MG	P-1-ME	100 pt 100 mm	100 to 100 to 100	Mary Services	District one		
44	- 3	D. C. TO	THE PERSON	10 0 Mg	10 p to 100	50 y 107 100	100 y 100 100	200		D. C. STO	
		A. p. mil	W. p. ani, ani,	K p to 1	April	25,912,105	N. p tal	100,000,000		N. y and	
Automa Trans	-										
IN.	100	D. H. ST.	PER STAR	STATE.	10.433.00	AND WATER	175,000	Part 176	21.00	No. of Parts	ALPER.
100	-		100 1 100 100			100 to 100	10.4 10.4				
			105.9 48.481			THE P SEA THE	OLD DE UNE				
STATE THE											
769	100	Part Action	TO A STATE	5 (50)	DATE:	FD 4 300 130	20 K SE 162	75 V 750 TO	A P MARK	To practice	FL (200)
NAME OF											
				ALC:	DATE			0.000	D 1/ 100		Division in
No.		2122	100 H 100 H	- num	Total Series	STATE OF THE	100, 41, 100, 1400	COLUMN TWO	2122	0.150	DIFFE
140	-	Ay THE	Director.	O y Mr.	20,000	MAN WAS THE	THE RELEASE	100-14 818-1700	PLE THE THE	n-yare	0,000,00

¹Supplemental Material. Table S1: Peak analyses of age clusters. Figure S1: Chondrite-normalized REE patterns in detrital zircon. Figure S2: LREE-HREE ratio plots. File S1: Detrital zircon U-Pb age data (this study and from Potter-McIntyre et al., 2016). File S2: U-Pb age peaks analysis. File S3: End Member analysis. File S4: Rare earth elemental geochemistry analysis in detrital zircon. File S5: Rare earth elemental geochemistry analysis in igneous zircon. Please visit https://doi.org/10.1130/GEOS.S.14471031 to access the supplemental material, and contact editing@geosociety. org with any questions.

(KDEs; bandwidth set at 10 m.y.) and histograms (bins discretized at 25 m.y.) (Fig. 5).

We used the Age Pick program, developed by the LaserChron Laboratory, to identify prominent age peaks, which were then used to quantitatively assess the spatial and temporal detrital zircon U-Pb age distributions of Middle–Upper Jurassic strata across the study sites. Age clusters of detrital zircons (age modes of three or more grains) and their respective proportions were calculated and grouped according to the age of source terranes in North America to assess their provenance (Table S1 and File S2 in the Supplemental Material¹).

We also measured the abundance of REEs in zircon (mostly from zircon cores using LA-ICPMS) from 316 grains (seven samples) that were previously analyzed for U-Pb age (File S4 [footnote 1]; Fig. S1). We estimated uncertainty by calculating the mean absolute deviation (MAD) of the individual analyses from the mean REE value (File S4). Trace element and REE abundances in detrital zircon grains were measured using a quadrupole LA-ICPMS at the University of Arkansas Trace Element and Radiogenic Isotope Laboratory (Fayetteville, Arkansas, USA). NIST612 glass was used as a primary standard, with NIST610 glass and the zircon Mud Tank used as secondary standards. Sample selection was based on the presence or absence of a Cambrian U-Pb age peak to assess the potential provenance of the Cambrian grains and, by extension, discriminate between the provenance of samples with this age peak and those without it (e.g., Potter-McIntyre et al., 2016). Within each of the seven samples, Cambrian grains were targeted for the purpose of comparing the REE abundances in detrital zircon with potential Cambrian igneous sources (File S5).

Trace elemental abundances and isotopic ratios in igneous zircons of Cambrian age were analyzed by a Varian 810 single-quadrupole inductively coupled plasma–mass spectrometer (ICPMS) equipped with a Photon Machine Analyte 193 laser at the University of Houston Texas, USA). Plešovice zircon (Sláma et al., 2008) and FCZ5 zircon from the Duluth gabbro complex (Paces and Miller, 1993) were used as internal and external zircon standards for fractionation correction in the U-Pb data,

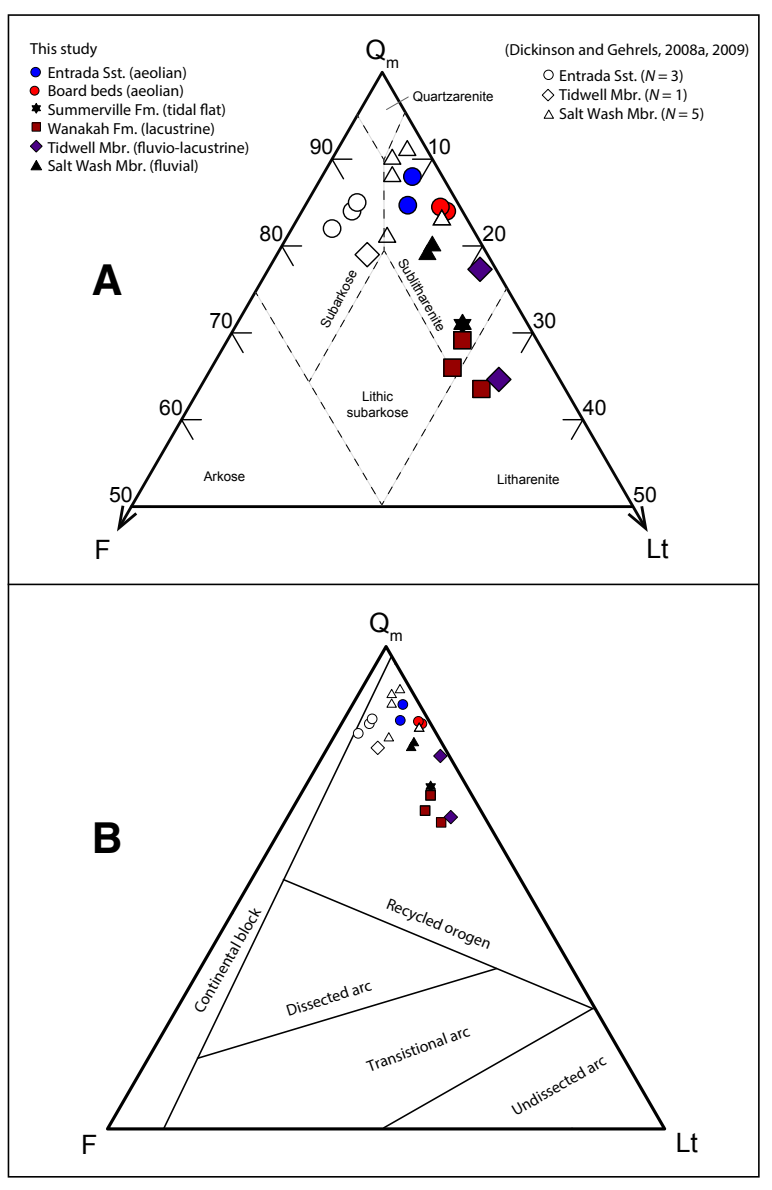


Figure 4. Sandstone and provenance classification plots using the methods of Dickinson and Suczek (1979). (A) Partial Ω_m -F-Lt (monocrystalline quartz grains–total feldspar–total lithic fragments) ternary plot of representative sandstone samples (Table 1) from the Paradox Basin. N is the number of samples. (B) Ω_m -F-Lt ternary plot of data in A. Petrographic data from Dickinson and Gehrels (2008a, 2009) are plotted for comparison, and the corresponding U-Pb detrital zircon data are plotted in Figure 11. See Table 1 for detrital modes of Ω_m -F-Lt grains. Sst. — Sandstone; Fm. — Formation; Mbr. — Member.

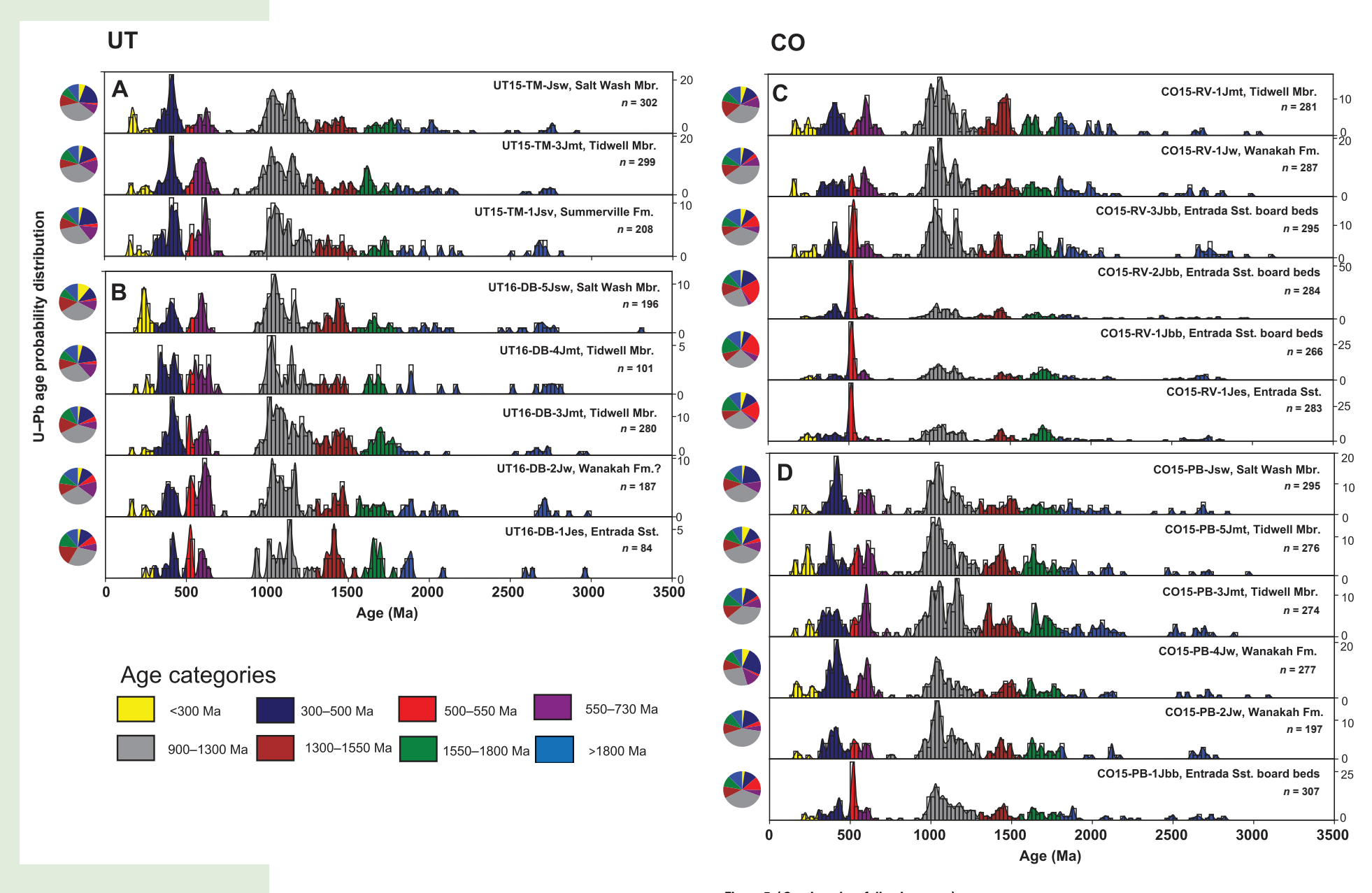
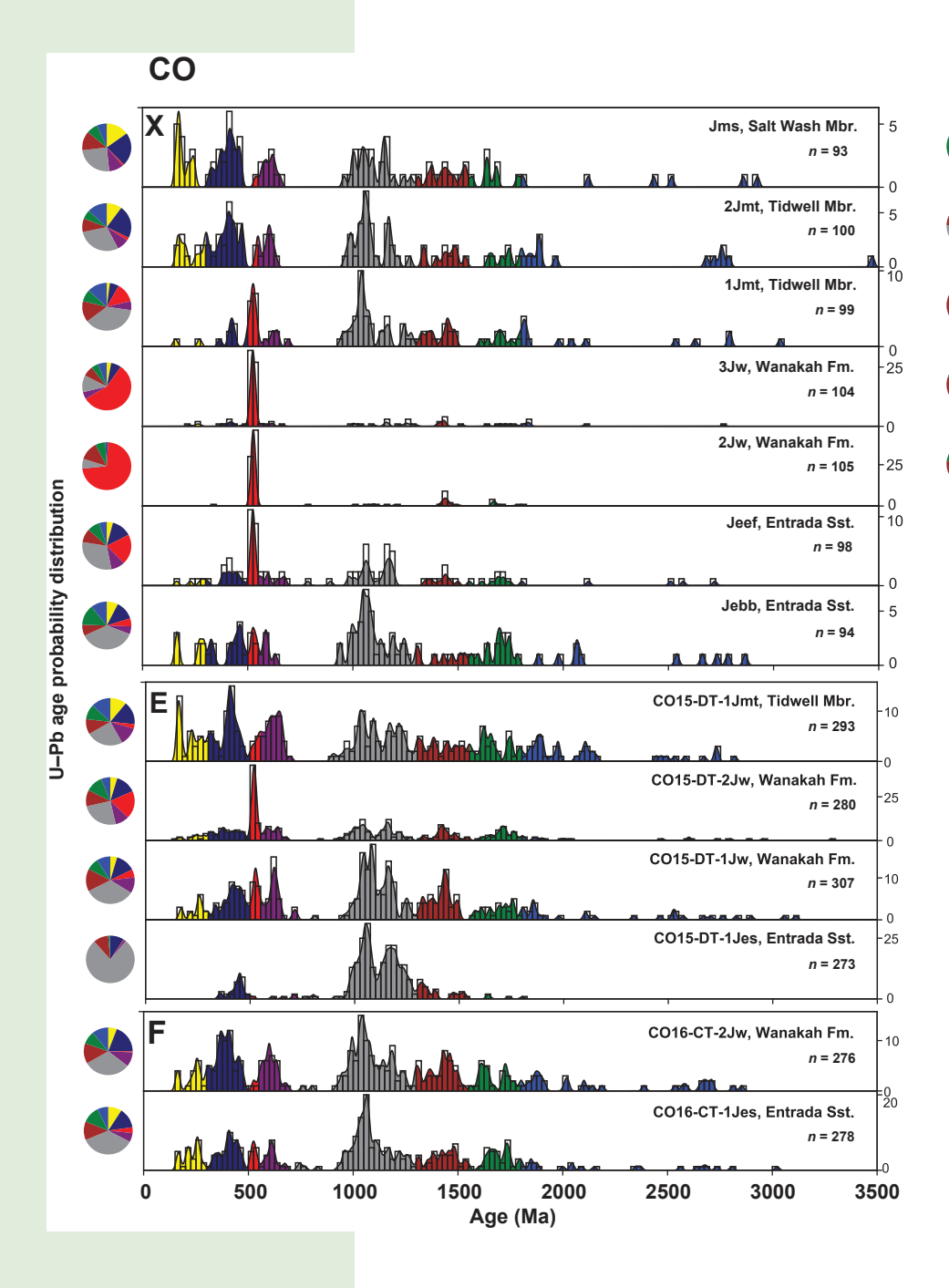


Figure 5. (Continued on following page.)



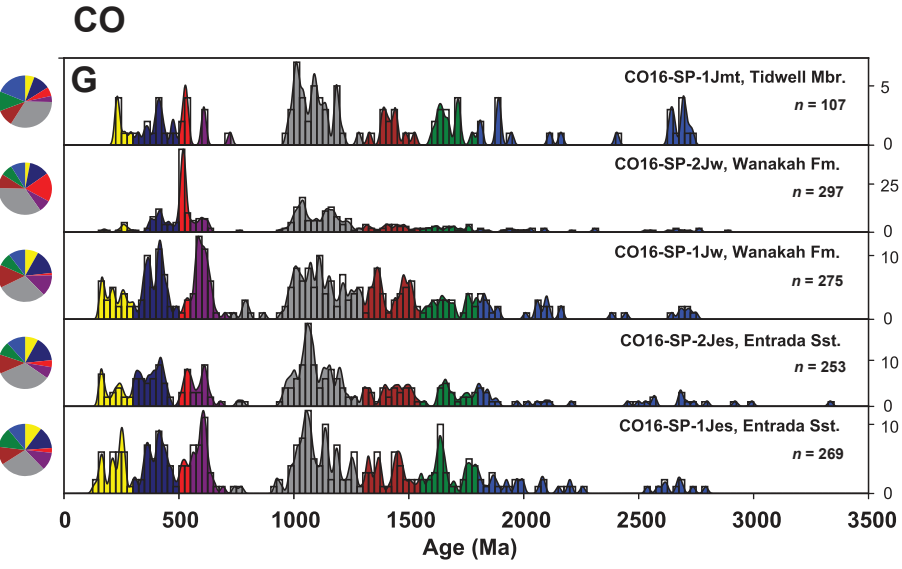


Figure 5. U-Pb detrital zircon ages of 31 sandstone samples from the Middle to Upper Jurassic strata in the Paradox Basin. Pie plots on the y-axis are the relative proportion of the age categories of detrital zircons. Study sites and stratigraphic horizons of the samples are shown in Figures 3 and 8, respectively. Histogram (bin size 25 m.y.) is perfectly superimposed with the kernel density estimate (KDE) plots (colored spectra with bandwidth 10 m.y.). n-number of zircon grains. KDEs of detrital zircon ages in the samples are plotted in stratigraphic order from oldest (bottom) to youngest (top), labeled with the sample number, and grouped according to study site (Fig. 3), generally from west to east (UT-Utah; CO-Colorado): A-Ten Mile Graben; B-Dewey Bridge; C-Rabbit Valley; D-Pollock Bench; E-Duncan Trail; F-Chukar Rail; G-Sawpit. Data in panel X are from Potter-McIntyre et al. (2016). X, Escalante Canyon, is a study site at the intersection of the east-west and southeast-northwest transect of the study sites from Chukar Trail and Sawpit, respectively, in the Paradox Basin (Figs. 3 and 8). Age distributions of zircon are plotted using detritalPy software (Sharman et al., 2018a). Mbr. - Member; Fm. - Formation; Sst. - Sandstone.

respectively. The NIST612 glass standard (Pearce et al., 1997) was used to correct trace element data. Zircon U-Pb data were reduced with lolite software (https://iolite.xyz), and ages were calculated using a Microsoft Excel macro, Isoplot 4.15 (https://sites.google.com/a/laserchron.org/laserchron/home). Trace element data were reduced and concentrations calculated with Glitter software (http://www.glitter-gemoc.com). Detrital and igneous zircon REE concentrations were normalized to chondrite values (McDonough and Sun, 1995).

Sediment Unmixing and End-Member Models

We applied the bottom-up sediment unmixing method to deconvolve the age distributions (i.e., daughters) into potential end members (EMs; parents) to better constrain the primary source rocks (Sharman and Johnstone, 2017; Saylor et al., 2019). We applied the non-parametric, non-negative matrix factorization (NMF) algorithm used by Paterson and Heslop (2015) to produce sets of EMs and their relative abundances from detrital zircon age distributions, which is similar to the numerical approach of unmixing grain-size distributions in sediments (e.g., Weltje, 1997; Weltje and Prins, 2003). We evaluated the goodness of fit of the NMF based on the percentage of the total data set variance (R^2) accounted for by the respective EM model and the angular deviation (θ) of the EMs from the original age distribution (Paterson and Heslop, 2015). The algorithm utilizes hierarchical alternating least-squares NMF (Lee and Seung, 1999) to produce a specified set of EMs and their abundances from a set of daughter age distributions. The best-fit mixture of EMs is reported as a set of mixing coefficients for each daughter sample, which allows evaluation of changing end-member abundance in space and/or time (Sharman and Johnstone, 2017).

By utilizing the NMF algorithm and the bottom-up sediment unmixing approach, we identified age distributions of end members that characterize parents (i.e., sources) that together could theoretically mix to form the multimodal age distributions observed in the new samples from this study and in seven samples from Potter-McIntyre et al. (2016) (Fig. 6; raw data in File S3 [footnote 1]). We produced four EM models composed of two to four end-member distributions for a broad assessment of the modeled parent distribution (Fig. 6) by running the NMF algorithm in a Matlab environment on a combined 8580 U-Pb ages from all 38 samples.

To determine the set of end members produced by the algorithm that provided the best fit of the original age distributions, we compared the goodness-of-fit statistics (i.e., R^2 and θ) of successive end-member sets, quantitative estimates, and visual inspection of the respective relative and cumulative probabilities of the U-Pb age distributions in the EM plots (Fig. 6). Unmixing U-Pb age distributions into potential end members has the advantage of reducing the inherent complexities associated with interpreting the heterogeneous age distributions without loss of their geologic significance.

RESULTS

Stratigraphic Correlation and Sandstone Petrofacies

Framework-grain and detrital modes from 12 representative aeolian, tidal, and fluvio-lacustrine sandstone samples are shown in Table 1 and Figure 4. The aeolian samples (Entrada Sandstone; Table 1A) are composed predominantly of very fine- to fine-grained, subrounded to rounded framework grains that are moderately well sorted. The samples are quartz rich (~84%–91%) with lithic fragment abundance ranging from 9% to 15%. The aeolian samples plot in the sublitharenite field of the $\rm O_m$ -F-Lt (monocrystalline quartz grains–total feldspar–total lithic fragments) diagram (Fig. 4A), based on the sandstone classification of Dickinson and Suczek (1979).

The tidal-flat sample (Summerville Formation; Table 1B), composed of poorly sorted, mediumgrained, angular to subangular framework grains, plots in the sublitharenite field on the Q_m -F-Lt diagram (Fig. 4A). The lacustrine (Wanakah Formation) and fluvio-lacustrine (Tidwell Member) samples

(Table 1C) are less quartzose and more feldspathic (potassium feldspar) compared to the other samples and plot in the sublitharenite and litharenite fields on the O_m-F-Lt diagram (Fig. 4A). Compared to the Entrada Sandstone samples, the Summerville, Wanakah, and Tidwell samples have a higher abundance of volcanic and metavolcanic lithic fragments (5%–10%; Tables 1B and 1C).

The petrofacies of the fluvial samples (Salt Wash Member) are similar to those of the eolianite samples (Table 1D) and are composed of fine-to medium-grained, moderately sorted, subrounded grains that plot in the sublitharenite field of the O_m -F-Lt diagram (Fig. 4A). A comparison of the detrital modes of sandstones from this new study with petrographic data from the same rocks in adjacent localities within the Colorado Plateau shows some similarity (Fig. 4A), except for the Entrada Sandstone which was classified as subarkose by Dickinson and Gehrels (2009).

U-Pb Detrital Zircon Data

Here we report a total of 7887 new detrital zircon U-Pb dates in addition to the 693 U-Pb ages from seven sandstone samples reported by Potter-McIntyre et al. (2016; Fig. 5). The average number of new detrital zircon U-Pb analyses per sample in this study is ~277, whereas the average is ~99 for the data published by Potter-McIntyre et al. (2016). Middle-Upper Jurassic detrital zircon age distributions from the Paradox Basin and the Central Colorado trough (CCT) are heterogeneous (Fig. 5). Major modes of zircon ages (average ≥15% of grains per sample) are present in three age ranges: 1.53-1.3 Ga, 1.3-0.9 Ga, and 500-300 Ma; minor but distinct modes (average ≤10% of grains) are present at 1.8-1.55 Ga, 730-540 Ma, and 540-500 Ma (Table S1). Seven sandstone samples are enriched (≤10% of grains) in Cambrian zircon with peak ages ranging from 530 to 512 Ma. Three of these samples have 22%-31% of the 540-500 Ma age mode, and the remaining four samples have lower abundances of Cambrian ages (10%-15%). We note the low proportion of Mesozoic zircon grains in our data set; these grains correspond to the Triassic-Early

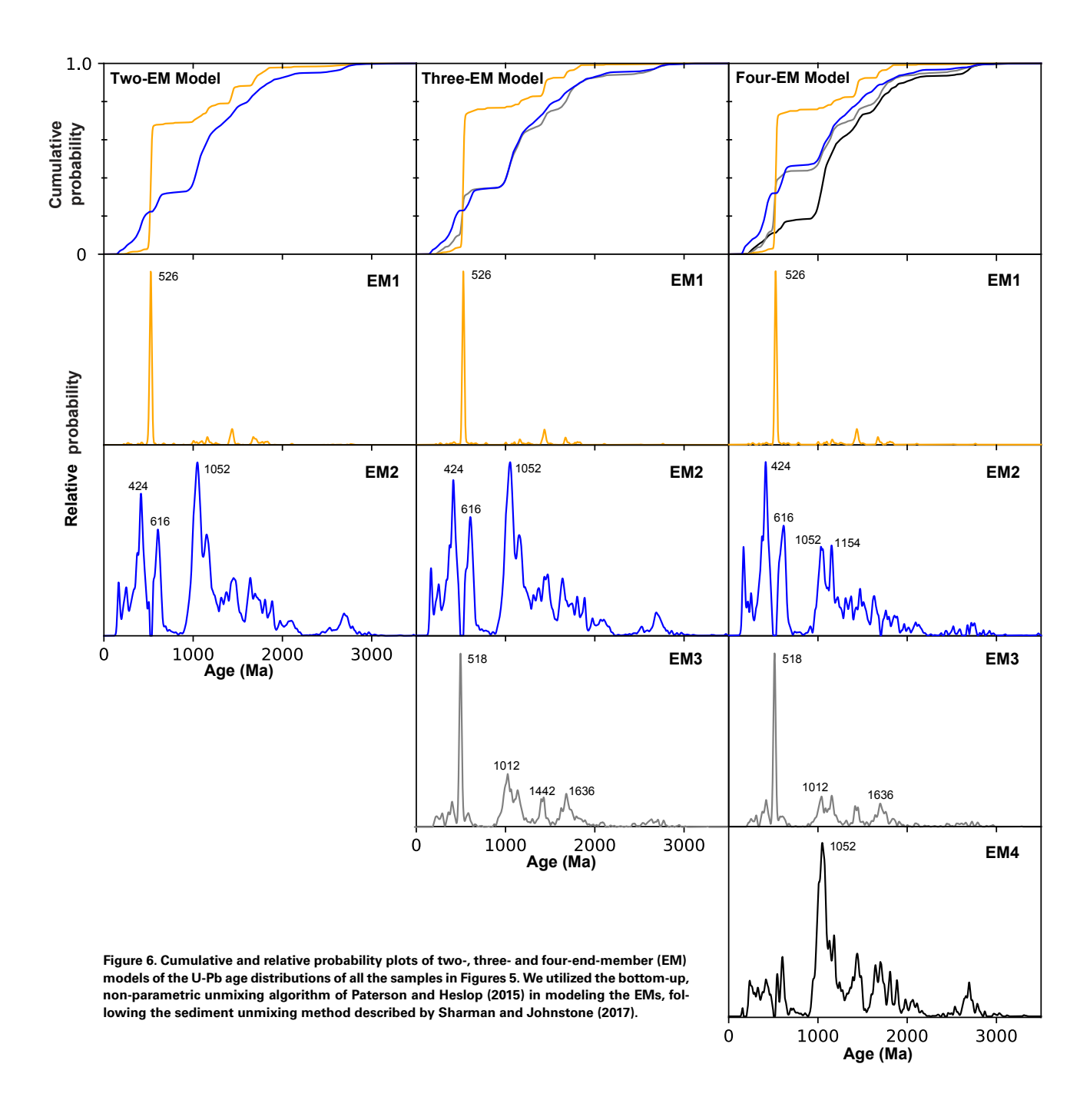


TABLE 1. MODAL COMPOSITIONS OF REPRESENTATIVE DETRITAL ZIRCON SAMPLES OF MIDDLE-LATE JURASSIC SANDSTONE IN THE PARADOX BASIN, WESTERN COLORADO AND SOUTHEASTERN UTAH

	A. Aeolian (Entrada Sandstone and board beds)				B. Tidal flat	C. Lacustrine and fluvio-lacustrine					D. Fluvial	
Grains	UT16-DB-1Jes	CO15-DT-1Jes	CO15-RV-2Jbb	CO15-PB-1Jbb	UT15-TM-1Jsv	UT16-DB-2Jw?	CO15-RV-1Jw	CO15-DT-2Jw	UT15-TM-3Jmt	UT16-DB-3Jmt	UT15-TM-Jsw	CO15-PB-Jsw
Q _m	88	83	84	85	70	66	61	65	64	75	79	80
Q_p	2	1	5	6	6	5	8	2	7	5	4	5
Q	90	84	89	91	76	71	69	67	71	80	83	85
Р	_	1	_	-	2	2	1	2	2	_	3	3
K	3	4	1	1	5	8	7	5	4	1	3	2
F	3	5	1	1	7	10	8	7	6	1	6	5
Lvm	1	3	3	2	7	6	5	9	10	6	3	3
Lsm	6	6	7	7	10	13	14	11	12	10	8	7
L	7	9	10	9	17	19	19	20	22	16	11	10
Lt	9	10	15	15	23	24	27	22	29	21	15	15

Note: See Figure 3 for sampling localities and Figure 8 caption for explanation of sample name abbreviations. Samples are listed east to west in each category except for the sample in column B. Detrital modes are reported in percentages based on point counts of >340 QFL (quartz-feldspar-lithic) framework grains per sample, excluding unclassified lithic fragments and accessory minerals. Monocrystalline grains: Q_m —quartz; P_m -plagicalse; P_m -potassium feldspar; P_m -total feldspar (P_m -total fragments; P_m -total fragments; P_m -total lithic fragments; P_m -total lithic fragments; P_m -total lithic fragments; P_m -total lithic fragments; P_m -total quartzose grains (P_m -total quartzose grains (P_m -total lithic fragments); P_m -total lithic fragments (P_m -total lithic fragments); P_m -total lithic fragments (P_m -total lithic fragments); P_m -total lithic fragments (P_m -total lithic fragments); P_m -total lithic fragments (P_m -total lithic fragments); P_m -total lithic fragments (P_m -total lithic fragments); P_m -total lithic fragments (P_m -total lithic fragments); P_m -total lithic fragments (P_m -total lithic fragments); P_m -total lithic fragments (P_m -total lithic fragments); P_m -total lithic fragments (P_m -total lithic fragments); P_m -total lithic fragments (P_m -total lithic fragments); P_m -total lithic fragments (P_m -total lithic fragments); P_m -total lithic fragments, P_m -total lithic fragm

Jurassic (ca. 241–181 Ma; \leq 6%) and Middle–Late Jurassic (ca. 175–145 Ma; \leq 4%).

Entrada Sandstone

The Entrada Sandstone samples (Jes; N=6, n=1113, where N is the number of samples and n is the total number of U-Pb grain analyses) each include at least four zircon age clusters: 1.8–1.55 Ga (~11%); 1.53–1.3 Ga (~13%); 1.2–0.9 Ga (~39%); and 500–300 Ma (~12%). A small (10%) group of 540–500 Ma grains with an ca. 523 Ma age peak is present in the Entrada Sandstone sample from Dewey Bridge, Utah. The Entrada Sandstone sample from Duncan Trail, Colorado, contains a higher abundance (~77%) of zircon ages between 1.2 and 0.9 Ga compared to the same unit from the adjacent Chukar Trail, Colorado, and other study sites (Figs. 3 and 5E; Table S1).

Board Beds of the Entrada Sandstone

Samples from the board beds unit of the Entrada Sandstone (Jebb; N=4, n=944) contain the four major age clusters found in the underlying Entrada Sandstone, plus the 540–500 Ma age

mode at higher abundances (~15%-31%) relative to samples from the underlying portion of the Entrada Sandstone (Figs. 5C and 5D; Table S1). The average percentage of zircon age clusters are ~11% for 1.8-1.55 Ga; ~11% for 1.53-1.3 Ga; ~29% for 1.2-0.9 Ga; ~21% for 540-500 Ma; and ~10% for 500-300 Ma. Prominent age peaks in the 540–500 Ma age group are present at 512 Ma and 516 Ma, while the 1.2-0.9 Ga age group shows two dominant peaks at 1041 Ma and 1030 Ma. The oldest and youngest peaks in the 1.2-0.9 Ga age group are present at 1165 and 1030 Ma, respectively. 540-500 Ma zircon with unimodal age peaks at 512 and 516 Ma account for ~30% of the board beds unit of the Entrada Sandstone at Rabbit Valley to the northwest of the Paradox Basin, while at Pollock Bench, the peak is at 520 Ma and 540-500 Ma zircon account for ~15% of the total (Figs. 5C and 5D; Table S1). At Escalante Canyon, the 540-500 Ma grains in the board beds unit have dominant age peaks between 527 and 519 Ma and constitute 11%-65% of the zircon grains.

Wanakah Formation

The sandstone samples from Wanakah Formation (Jw; N = 9, n = 1968) are characterized by a

mixture of three main zircon age clusters: 500-300 Ma (~17%), 1.3–0.9 Ga (~34%), and 1.53–1.3 Ga (~13%). However, the Wanakah Formation also contains abundant 540-500 Ma zircon (6%-22%), with age peaks present between 529 and 512 Ma. At Escalante Canyon, age peaks are present at 527 and 523 Ma in the lower and upper sandstone units of the Wanakah Formation, respectively, with 540-500 Ma zircon accounting for 55%-65% of the total (Fig. 5X; Table S1). At Sawpit and Duncan Trail, 540-500 Ma zircon composes 22% of the Wanakah samples with an age peak at 519 Ma. Samples from the west and northwest of the study area, within the Paradox Basin, have lower abundances of 540-500 Ma zircon (2%-31%) relative to the corresponding samples in the CCT.

The U-Pb ages from a thin (~0.2–0.3 m) calcareous sandstone bed (hypothesized as the basal Wanakah Formation based on field observations) that overlies the massive Entrada Sandstone at Dewey Bridge, Utah, are broadly similar to those observed in the Wanakah Formation in other study sites in western Colorado (Fig. 5B; Table S1). This basal Wanakah Formation sample has elevated proportions of <300 Ma grains (2%), 730–540 Ma grains (14%), and grains with ages between 3.2 and 2.4 Ga and between 2.3 and 2.0 Ga (4% each).

Summerville Formation

Four major U-Pb age clusters characterize the detrital zircon distributions in the Summerville Formation sample (Jsv; N=1, n=156): 1.53–1.3 Ga (~14%) with peaks at 1461 and 1320 Ma; 1.3–0.9 Ga (~31%) with major peaks at 1219 and 1050 Ma; 730–540 Ma (~18%) with a peak at 620 Ma; and 500–300 Ma (~20%) with peaks at 355 and 414 Ma (Fig. 5A; Table S1). Minor peaks at 1840 Ma and 1965 Ma are present within the 2.0–1.8 Ga age cluster that forms ~7% of the total grain distribution.

Tidwell Member of the Morrison Formation

The Tidwell Member (Jmt) of the Morrison Formation is widespread across the Paradox Basin. Sandstone samples (N = 8, n = 1560) from the Tidwell Member contain four sets of age clusters that vary in abundance from the southeastern section of the Paradox Basin to the northwest and east (Table S1). At Sawpit, Colorado, the basal sandstone of the Tidwell Member contains three main age clusters at 3.2-2.4 Ga (~11%), 1.8-1.55 Ga (~14%), and 1.3–0.9 Ga (~38%). Minor age clusters are also present at ages 2.0-1.8 Ga (~8%) and 1.53-1.3 Ga (~9%). The respective peaks of these age clusters are shown in Table S1. At the northwestern (Pollock Bench, Colorado) and eastern (Ten Mile Graben, Utah) sections of the Paradox Basin (Figs. 3) and 5), the detrital zircon grains in the Tidwell Member samples include significant proportions of the 1.53-1.3 Ga (~9%-15%), 730-540 Ma (18%), and 500-300 Ma (~12%-21%) age clusters. The 1.3-0.9 Ga age cluster is the most dominant (average proportion of ~34%) in the Tidwell Member samples and appears consistent across the Paradox Basin and CCT, similar to the Wanakah Formation and Entrada Sandstone samples (Fig. 5; Table S1). The Upper Jurassic Tidwell Member has lower abundances of 540-500 Ma grains relative to the underlying Middle Jurassic Wanakah Formation. For example, at Escalante Canyon, 540-500 Ma grains constitute only ~11% of the Tidwell Member sample (peak age of 523 Ma) compared to 55% and 65% of the Wanakah Formation samples (Fig. 5X; Table S1). At Dewey Bridge, 540–500 Ma zircon form 5%–6% of two Tidwell Member samples, with the lower sample having a distinctive age peak at 520 Ma. At Sawpit, 540–500 Ma zircon account for 7% of the total, with a peak age of 526 Ma that is similar to that of the underlying Wanakah Formation (519 Ma). Tidwell Member samples from all other sections have low abundances of 540–500 Ma zircon (3%), similar to the overlying Salt Wash Member.

Salt Wash Member of the Morrison Formation

The U-Pb age distributions of zircon grains in Salt Wash Member samples (Jsw; N = 3, n = 611) from Ten Mile Graben and Dewey Bridge (both in Utah) and Pollock Bench, Colorado, show two primary age clusters: 1.3-0.9 Ga (~29%-35%) and 500-300 Ma (~15%-23%). Also, significant proportions of zircon grains from the 1.8-1.55 Ga (~8%-9%), 1.53-1.3 Ga (~10%-17%), and 730-540 Ma (~11%-14%) age clusters are present in these samples (Table S1). The proportion of 1.3-0.9 Ga grains in the Salt Wash Member samples increases to the east across the Paradox Basin, while the abundance of 730-540 Ma grains decreases concomitantly. The three Salt Wash Member samples either lack the distinctive 527-519 Ma peak found in underlying samples or display a low abundance of 540-500 Ma zircon (2%).

End-Member Analysis

The end-member (EM) analysis was conducted on a combined data set of detrital zircon U-Pb age distributions in all 38 samples from the Paradox Basin and Central Colorado trough (31 from this study and seven from Potter-McIntyre et al. [2016]). The *R*² for the two-, three-, and four-EM models are 85.4%, 88.3%, and 89.9%, respectively, while the corresponding θ values are 20.3°, 18.0°, and 16.7°. Given the very modest improvement in *R*² between three-EM and four-EM models, and to avoid potential overinterpretation of the EM analysis results, we focus our analysis below on the two-EM and three-EM cases (Fig. 6).

We note from the EM plots that: (1) EM1 has a mode at 526 Ma that accounts for 74%-76% of

the total EM age distribution; (2) EM2 has a major peak at 1052 Ma and additional peaks at 1154, 424, and 616 Ma; (3) EM3 displays a prominent peak at 518 Ma, and also contains several other age peaks including at 1636, 1442, and 1012 Ma that together constitute 8%–10% of the total; and (4) the major age peaks of EM4 in the four-EM model have already been accounted for in EM2 of the preceding three-EM model. We exclude results of the EM4 model in our discussion because it provides little additional context to our data set.

Zircon Rare-Earth Elements (REEs)

The REE concentration in zircon reflects the composition of the magma from which an individual zircon crystallized and can be used as an additional proxy for provenance (e.g., Belousova et al., 2002). The chondrite-normalized, mean REE patterns of Cambrian detrital zircon from seven sandstone samples and in the Cambrian zircon from five potential igneous sources are plotted in Figure 7. Figure S1 includes plots of chondrite-normalized, mean REE patterns in all the detrital grains from 316 analyses. The REE abundances in the Cambrian and non-Cambrian grains are similar, and there is no systematic variation in REE patterns between the samples with a major or a minor Cambrian peak. The Cambrian grains constitute between 43% and 64% of the total number of grains in three samples (CO15-PB-1Jbb, CO15-RV-2Jbb, and CO16-SP-2Jw) and between 12% and 20% in four samples (CO15-PB-3Jmt, CO15-RV-1Jw, CO16-SP-1Jes, and UT15-TM-Jsw) (Fig. S1; File S4 [footnote 1]).

The mean REE concentrations of Cambrian zircon for each sandstone sample (average value of 4–32 analyses per sample) are shown in Figure 7A. The MAD values indicate a significant variation of individual REE concentrations in Cambrian zircon within the same sample. Overall, MAD values show less intrasample variation in the light REE (LREE) to middle REE (MREE) concentrations (La–Tb) in all samples (dispersion from the mean REE value is mostly <20%), while the heavy REE (HREE) concentrations (Dy–Lu) show significant intrasample

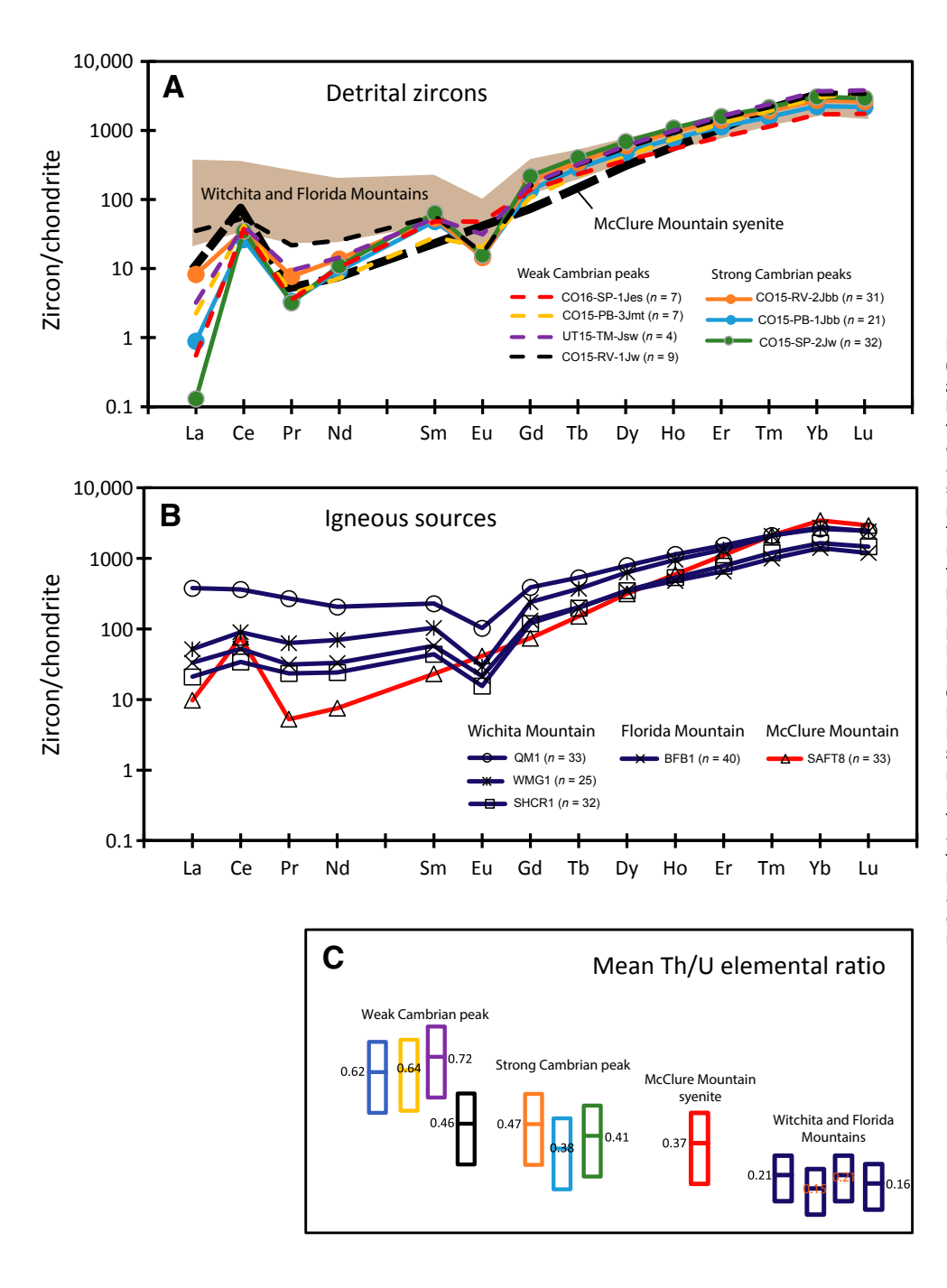


Figure 7. A comparison of rare-earth element (REE) concentration in detrital and igneous zircon. (A) Plots of chondrite-normalized mean **REE concentrations in Cambrian detrital zircons** from seven sandstone samples from the Paradox Basin (this study). Solid lines with markers are REE patterns in zircons from the sandstone samples (N = 3) that display a major Cambrian peak, and dashed lines without markers are from the sandstone samples (N = 4) that have minor or no Cambrian peak (see Fig. 8 caption for explanation of abbreviations used in sample names). (B) Mean REE concentrations (open markers with solid lines) of Cambrian zircons per sample from five potential igneous sources in Colorado (CO), New Mexico (NM), and Oklahoma (OK): QM1-Quartz Mountain granite, Oklahoma; WMG1-Mount Scott granite, Oklahoma; SHCR1-Slick Hills rhyolite, Oklahoma; BFB1-Florida Mountain syenite, New Mexico; SAFT8-Wet Mountain nepheline syenite, Colorado. (C) Box plots showing relative mean Th/U ratios in detrital and igneous Cambrian zircons from samples in A and B for comparison. Values at the middle of the box plot in panel C represent the mean Th/U ratio, and the top and bottom lines are the upper and lower limits of the deviation from the mean value. n-number of zircon grains per sample. Chondrite normalization values are from McDonough and Sun (1995).

variations with dispersion from the mean REE value >50%.

The chondrite-normalized mean REE patterns of all detrital zircon from this study are broadly similar, excluding several zircon grains from one sample (i.e., CO15-RV-1Jw) that display a nearly flat LREE pattern. The HREE patterns in all samples significantly overlap in their relative abundance (Fig. 7A) but are somewhat distinct from the REE patterns of Cambrian zircon from potential igneous sources in Laurentia (Fig. 7B). Some potential sources of Cambrian zircon in Laurentia include the McClure Mountain syenite (sample SAFT8; 523 ± 0.12) of the Wet Mountains, central Colorado (Schoene and Bowring, 2006); diabase dikes in west-central Colorado (Larson et al., 1985); the Cambrian rhyolitic and granitic provinces of the Southern Oklahoma aulacogen (Hogan and Gilbert, 1998; Hanson et al., 2009), which includes the Wichita Mountains, Oklahoma (525 ± 25 Ma), comprising the Quartz Mountain granite (sample QM1), the Slick Hills rhyolite (sample SHCR1), and the Mount Scott granite (sample WMG1) (Powell et al., 1980); and Florida Mountain syenite (sample BFB1; 504 ± 10 Ma) in southwestern New Mexico (Geissman et al., 1991).

The REE patterns of detrital zircon in the sandstone samples show strongly depleted LREEs (La-Nd), a moderate abundance of MREEs (Sm-Tb), and a progressive enrichment of HREEs (Dy-Lu) (Fig. 7A). These detrital zircon grains have a positive Ce anomaly, a negative Eu anomaly, and a slightly concave-down curvature of the HREE pattern (Fig. 7A). In contrast, the LREEs of the Wichita Mountains and Florida Mountains samples are more enriched than in the detrital samples, while the HREEs in both the detrital and igneous zircon overlap (Figs. 7A and 7B). Zircon from granitic sources in the Wichita Mountains (i.e., samples QM1 and WMG1) are more enriched in overall REE content, while zircon from the rhyolite (sample SHCR1) and syenite (samples BFB1 and SAFT8) igneous sources are the most depleted (Fig. 7B). The La (chondrite-normalized) values of the igneous zircon (0.99-2.58) are several orders of magnitude higher than those of the detrital zircon (0.05-1.55) (File S4 and S5 [footnote 1]).

The REE patterns of detrital and igneous zircon grains have a negative slope, i.e., (La/Lu)_N values for the detrital zircon range from -2.0 to -4.3 and those for the igneous zircon range from -0.8 to -2.5 (File S4 [footnote 1]). The vertical bars in the previous paragraph represent the absolute value of the chondrite-normalized element while the parenthesis is the chondrite-normalized values of the elemental ratio. Eu/Eu* (asterisk represents Eu anomaly) values for the detrital zircon range from -0.23 to -0.87 and are somewhat comparable to those of the igneous samples from the Wichita Mountains, which range from -0.46 to -0.73 (File S4). The Th/U ratio for Wichita Mountains igneous zircon is lower than that of the detrital zircon, and this ratio in the Cambrian zircon from detrital samples that display a Cambrian peak is lower (0.38–0.47) than in the samples that have few Cambrian zircon grains (0.46-0.72) (Fig. 7C; File S4). The Th/U ratio for samples from the Wichita Mountains are lower (0.16-0.21) than that of the McClure Mountain syenite sample (0.37) (Fig. 7C; File S4). The Ce/Gd ratio in the detrital and igneous zircon is <0.4, excluding samples QM1 and SAFT8 with ratios of 0.93 and 1.03, respectively; the Nd/Gd ratio for the detrital zircon is <0.2 and for the igneous zircon is <0.5; and the Gd/Yb ratios for the detrital and igneous zircon are <0.2 (Fig. S2; File S4).

DISCUSSION

Detrital Zircon Sources in Laurentia

The U-Pb age distributions of detrital zircon in most of the samples (Figs. 5 and 8) are comparable with those of previously published samples from Jurassic rocks of the Colorado Plateau region (e.g., Bickford et al., 1989; Dickinson and Gehrels, 2003, 2008a, 2010; Schoene and Bowring, 2006; Potter-McIntyre et al., 2016). The original bedrock source of detrital zircon to the Entrada, Wanakah, Summerville, and Morrison formations in the Paradox Basin can be inferred via comparison with known Laurentian basement age domains (Fig. 9).

Three major age clusters of zircon grains are consistently present in the Middle–Upper Jurassic

sedimentary strata deposited in the Paradox Basin and Central Colorado trough (CCT): 1.53-1.3 Ga, 1.3-0.9 Ga, and 500-300 Ma. The 1.53-1.3 Ga zircon reflect ultimate derivation from the Mesoproterozoic anorogenic granite-rhyolite igneous provinces that intruded the Laurentian midcontinent and extend to northeastern Laurentia (Fig. 9). The 1.3-0.9 Ga grains reflect zircon originally derived from the Mesoproterozoic to early Neoproterozoic Grenville basement (Dickinson and Gehrels, 2003, 2008b, 2009). The 500-300 Ma zircons are characteristic of zircon primarily derived from the Appalachian orogen or peri-Gondwanan terranes in southeastern Laurentia, which consist of synorogenic Paleozoic rocks that span three orogenies: the Taconic (490-440 Ma), Acadian (420-350 Ma), and Alleghenian (330-270 Ma) (Fig. 9; Thomas, 2011).

Neoproterozoic (730–540 Ma) zircon could have been derived originally from sources lying to the southeast, such as the accreted southeastern fringe of Gondwanan terranes (ca. 680–530 Ma) and/or lapetan rift plutons (ca. 760–530 Ma) incorporated into the Appalachian orogen (Dickinson and Gehrels, 2010). The abundance of Cambrian detrital zircon (age peaks from 527 to 512 Ma) in sandstones from the Middle Jurassic Entrada Sandstone and Wanakah Formation and Upper Jurassic Tidwell Member of the Morrison Formation across the study sites is enigmatic (Figs. 5 and 8).

Sediments Recycled from Older Strata

Provenance classification from sandstone petrography (Fig. 4B) and detrital zircon ages (Fig. 5; Table S1) suggests that sediments deposited in the Paradox Basin and CCT during Middle–Late Jurassic time originated from multiple orogenic sources and/or from the recycling of grains through older strata that were derived from multiple sources. Recycling of zircon grains (Fig. 4B), particularly those of Grenvillian age, is plausible given that all samples (this study and previous work) plot in the "recycled orogen" provenance field (Fig. 4B) of Dickinson and Suczek (1979) and that multiple sediment-transport processes delivered sediment to the basin. We invoke two potential reasons for the

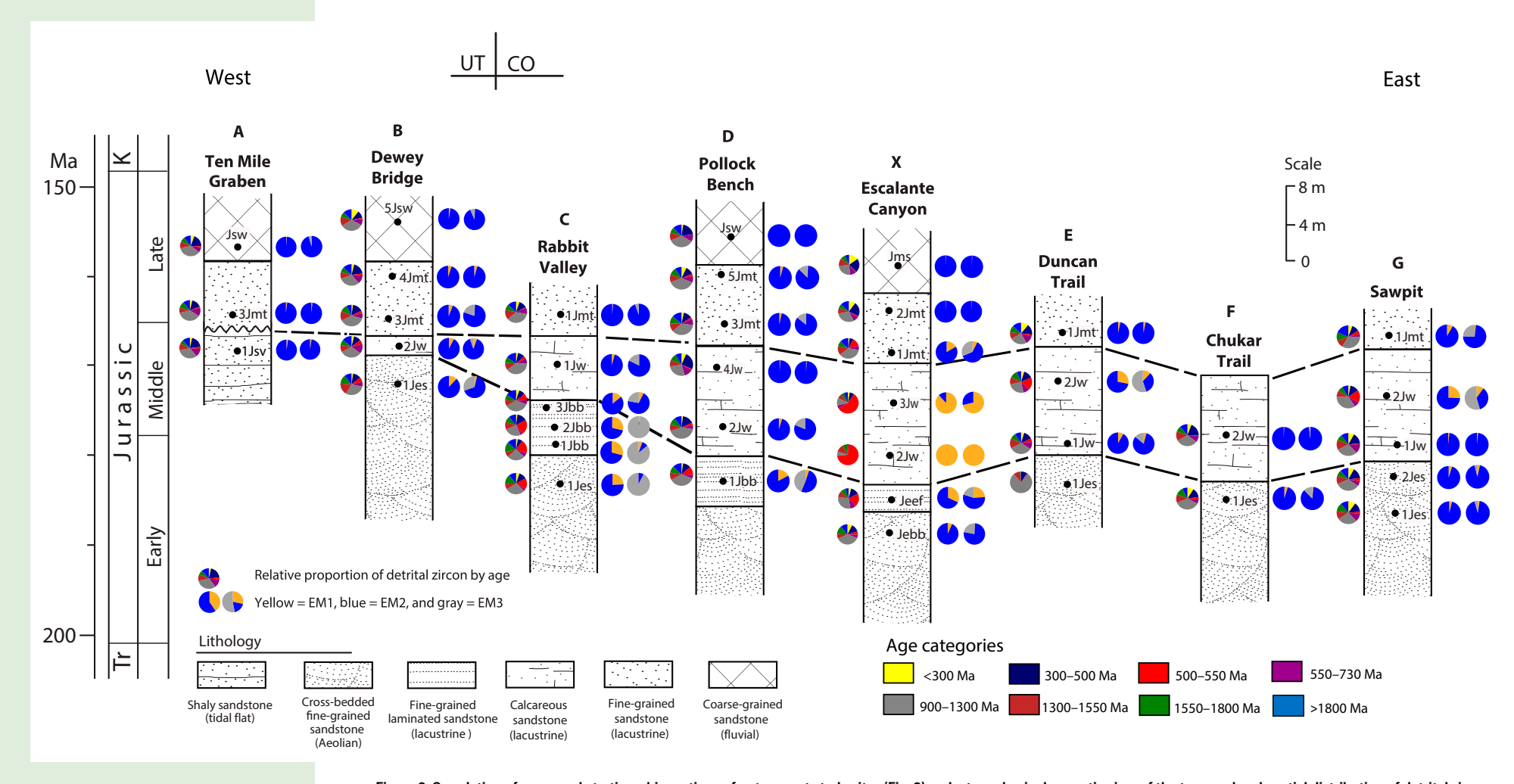


Figure 8. Correlation of measured stratigraphic sections of outcrops at study sites (Fig. 3) and a trans-basinal synoptic view of the temporal and spatial distribution of detrital zircon U-Pb ages within the Paradox Basin. Pie plots show the relative proportion of detrital zircon ages for the real (pie plots on the left side of each stratigraphic column) and two- and three-end-member (EM) modeled (pie plots on the right side of each stratigraphic column) age distributions. Sample abbreviations: J—Jurassic; sv—Summerville Formation; es—Entrada Sandstone; ebb, bb—board beds of the Entrada Sandstone; w—Wanakah Formation; mt, sw—Tidwell and Salt Wash Members of the Morrison Formation; ms—Salt Wash Member of the Morrison formation; eef—Wanakah Formation. The wavy line in column A between the Summerville Formation and the Tidwell Member of the Morrison Formation at Ten Mile Graben represents the J-5 unconformity. Other abbreviations: UT—Utah; CO—Colorado; Tr—Triassic; K—Cretaceous.

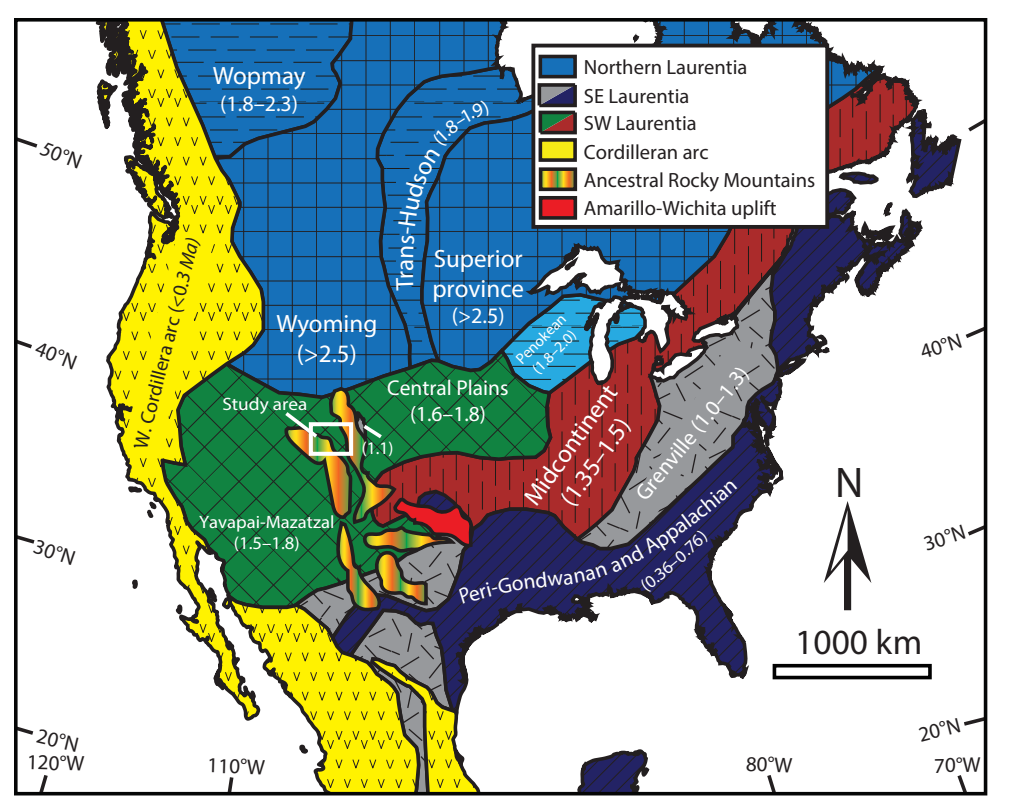


Figure 9. Location and approximate extent of basement age provinces in Laurentia. Primary source regions for detrital zircons deposited in the sedimentary rocks in North America are color-coded to match the age distributions of zircon grains shown in Figure 5 (Dickinson and Gehrels, 2009; Fildani et al., 2016; Sharman et al., 2018b). Basement ages shown in the map are in Ga.

similarity in U-Pb age distributions in Middle–Upper Jurassic strata: (1) confluence of drainages linking multiple source localities that were exhumed and eroding during Mesozoic time in southwestern Laurentia (Figs. 2 and 10), and (2) recycling and mixing of older sedimentary units with primary sediments from igneous sources (Thomas, 2011; Schwartz et al., 2019).

The sediment unmixing approach highlights the main end-member (EM) provenance signatures (Fig. 6) along with the relative EM abundances in sandstone samples (Fig. 8; File S3 [footnote 1]). The age modes and EM abundances of EM1 and

EM3 of the three-EM model (Fig. 6) highlight the spatial and temporal distribution of the anomalous Cambrian zircon. EM2 contains age peaks that are abundant throughout most samples and thus are interpreted to represent a background U-Pb age signature (Fig. 8). EM1 has a pronounced 526 Ma peak and is abundant only in a few samples of the Middle Jurassic Entrada Sandstone and Wanakah Formation, particularly at Escalante Canyon, but wanes in the Upper Jurassic Morrison Formation (Fig. 8). EM3 has a slightly younger Cambrian peak (518 Ma) relative to EM1 and is variably present in the uppermost Entrada Sandstone to Tidwell Member of the

Morrison Formation in all studied sections except the westernmost and easternmost sections (Ten Mile Graben and Chukar Trail, respectively; Fig. 8). The peaks in EM1 and EM3 suggest the Cambrian grains originate from more than one igneous source. The abundances of EM1 and EM3 are greatest at Escalante Canyon and appear to decrease toward the west and east (Fig. 8). The abundance of Cambrian zircon within a southeast-northwest transect across the CCT suggests that a route of northwest-flowing sediment transport occurred during the Middle Jurassic in western Colorado (Figs. 3 and 8). This sediment dispersal pattern is similar to that of the Eagle paleoriver inferred for the older (Late Triassic) Chinle-Dockum system (Dickinson and Gehrels, 2008b). Differences in the abundances of Cambrian grains between the study sites in the east versus the west may be explained by the presence of a drainage divide between the Paradox Basin and the CCT (Fig. 10). Potentially, the remnant of the southeast-northwest-trending Ancestral Front Range and associated structural features within the vicinity of the CCT may have partitioned the basin, effectively forming barriers that rerouted sediments to the CCT (Figs. 3 and 10). Alternatively, the reworking of sediments from the Entrada Sandstone into the Wanakah Formation at Escalante Canyon (inferred as the depocenter) from the east and west is plausible. Given that the Wanakah Formation is lacustrine, there are no paleocurrent indicators in the outcrop to either support or refute this hypothesis.

Provenance of Cambrian Grains

The provenance of detrital zircon grains may be constrained by comparing their REE chemistry with that of igneous zircon from potential sources (e.g., Belousova et al., 2002; Hoskin and Schaltegger, 2003). Although zircon grains typically exhibit intragrain and intergrain compositional and geochemical variations within a given distribution (e.g., Armbrustmacher, 1984; Hoskin and Ireland, 2000; Chapman et al., 2016), the enrichment or depletion of LREEs versus HREEs, presence or lack of REE proxies (e.g., chemical anomalies), and overall

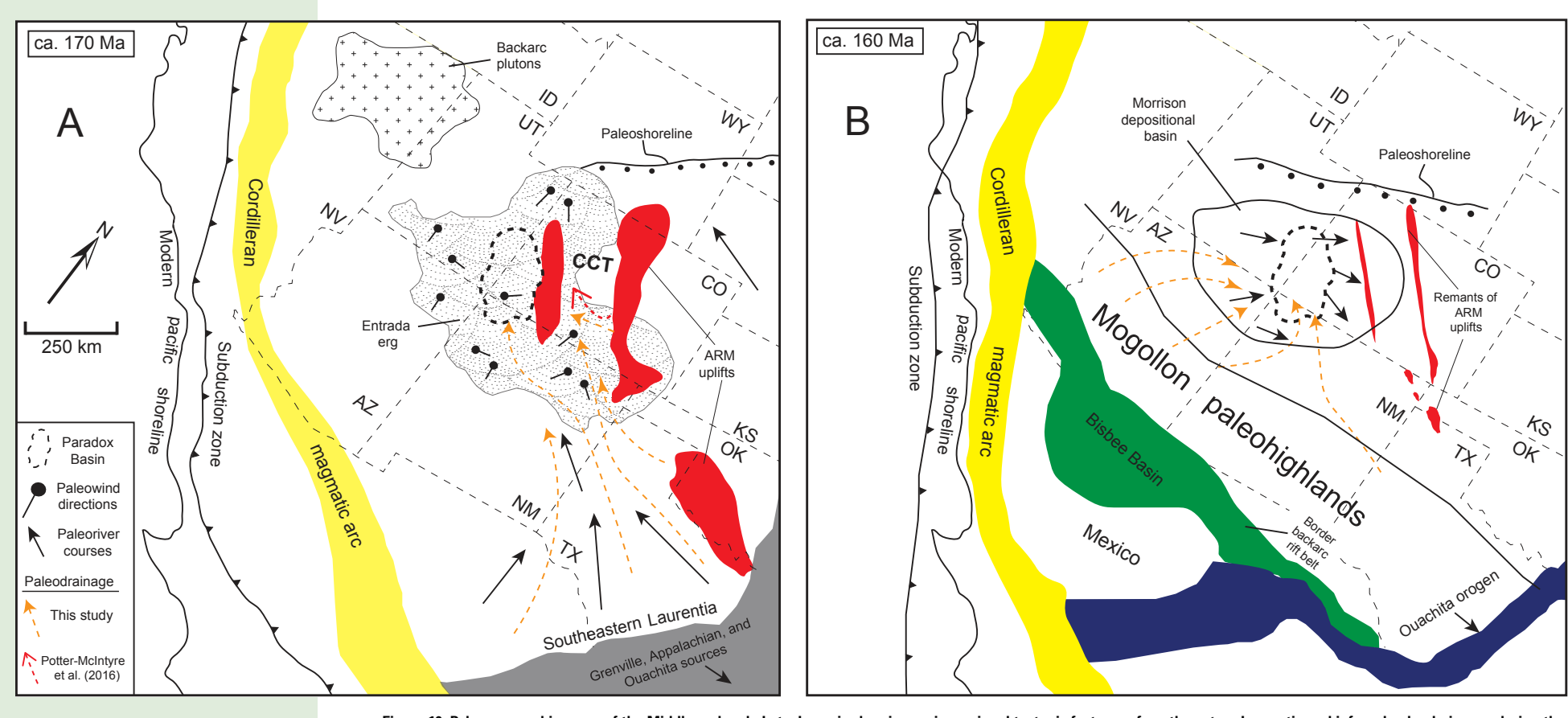


Figure 10. Paleogeographic maps of the Middle and early Late Jurassic showing major regional tectonic features of southwestern Laurentia and inferred paleodrainages during the deposition of the Mesozoic strata in the Paradox Basin and the adjacent Central Colorado trough (CCT). (A) Map at ca. 170–162 Ma (Bajocian–Callovian) corresponding to the period of widespread aeolian processes (the Early to Middle Jurassic ergs) on the Colorado Plateau and subsequent evolution of the lacustrine Wanakah Formation. (B) Map at ca. 160–155 Ma (Oxfordian) corresponding to the fluvio-lacustrine deposition of the lower Morrison Formation (Tidwell Member) and the fluvial systems of the Salt Wash megafan (upper Morrison) and correlative strata that evolved during the Late Jurassic deposition in southwestern Laurentia. Paleogeographic maps are modified after Peterson (1994), Dickinson and Gehrels (2010), and Blakey (2012). Dashed lines with arrows represent paleodrainages: orange—inferred from this study; red—Potter-McIntyre et al. (2016). Long black arrows in A represent transcontinental paleoriver courses, while short black arrows in B represent fluvial paleocurrents. Middle Jurassic paleowind directions, fluvial paleocurrents, transcontinental paleoriver courses, and paleotectonic features of southwestern Laurentia are compiled from Peterson (1988), Dickinson and Gehrels (2008a, 2009, 2010), and Blakey (2012). ARM–Ancestral Rocky Mountains. State boundaries are marked by dashed lines: NV—Nevada; ID—Idaho; UT—Utah; AZ—Arizona; WY—Wyoming; CO—Colorado; NM—New Mexico; KS—Kansas; OK—Oklahoma; TX—Texas.

pattern of the REE chemistry in the detrital and igneous zircon provide important insights in evaluating provenance. Although Cambrian zircon grains are found in samples thought be sourced from peri-Gondwanan and/or Appalachian terranes (Nance et al., 2002; Dickinson et al., 2010), such samples are not known to contain the high proportion of 540-500 Ma grains present in some of our samples. Also, the lack of Neoproterozoic and Paleozoic age fractions in the samples hosting abundant 540-500 Ma zircon does not support a peri-Gondwanan and/or Appalachian source. Cambrian zircon may also be recycled from older sedimentary assemblages (e.g., the Triassic Chinle-Dockum Group; Dickinson and Gehrels, 2008b; Dickinson et al., 2010).

The mean Th/U ratios of Cambrian detrital zircon range from 0.38 to 0.72 (File S4 [footnote 1]), which is typical of zircon of igneous origin (Hoskin and Ireland, 2000). However, mean Th/U ratios from samples with the distinctive Cambrian age peak (0.38–0.47) are more similar to that of the McClure Mountain syenite sample (0.37) versus those of samples from the Wichita Mountains of Oklahoma (0.16–0.21) (Fig. 7). The REE data for zircon in the samples with and without the distinctive Cambrian age peak have a similar pattern of HREEs (Dy–Lu), but the LREE (La–Nd) pattern is variable, with some samples exhibiting patterns similar to those observed in zircon from the igneous sources (Figs. 7A and 7B; Figure S1).

The REE concentrations as observed in our samples highlight the type of magma the zircon grains crystallized from (e.g., Armbrustmacher, 1984; Chapman et al., 2016) but do not ultimately prove their provenance given the high variability in REE concentrations (Fig. S2; Hoskin and Ireland, 2000). The positive Ce anomaly, enrichment of HREEs over LREEs, negative Eu anomaly (excluding sample SAFT8 from the McClure Mountain syenite), and the nearly consistent REE pattern plots (Fig. 7) suggest the detrital zircon grains are primarily magmatic, not metamorphic, and have not undergone significant alteration due to metamictization (Hoskin and Ireland, 2000; Rubatto, 2002). Igneous samples from the Wichita Mountains all display a weak Ce anomaly, but the pronounced

Ce anomaly in zircon sample SAFT8 (McClure Mountain syenite) (Fig. 7B) is characteristic of zircon derived from a syenitic source, while zircon from granitoid, carbonatite, and kimberlite sources typically have small to moderate Ce anomalies (Belousova et al., 2002). The Cambrian detrital zircon from all seven detrital samples are characterized by a high Ce anomaly that is more similar to that of the McClure Mountain syenite than to that of the igneous sources from the Wichita Mountains (Fig. 7A).

The negative Eu anomalies exhibited by the detrital and igneous zircon, excluding zircon sample SAFT8 which has no Eu anomaly (Fig. 7), are signature features of zircon derived from granitic source rocks and are indicative of either a parent magma that was depleted in Eu (Schaltegger et al., 1999) or zircon that concurrently crystallized along with the K-feldspar mineral phase, an Eu sink (Hinton and Upton, 1991). While the large positive Ce anomaly of igneous zircon sample SAFT8 is also observed in sandstone samples with both major and minor Cambrian zircon distributions, igneous zircon sample SAFT8 lacks the Eu anomaly that is observed in all detrital samples. Some aspects of the REE pattern (i.e., a steady enrichment of HREEs and a negative Eu anomaly) of the Wichita Mountains igneous sources in the southeast and the LREE pattern of the McClure Mountain syenite seem to correlate with the REE pattern of the detrital zircon samples (Fig. 7A).

The U-Pb age of Cambrian zircon from the McClure Mountain syenite has been well documented (e.g., Schoene and Bowring, 2006; Pivarunas and Meert, 2019), but findings from this study raise the question of whether the McClure Mountain syenite alone would have been able to account for the abundance of Cambrian grains found in the Entrada Sandstone and Wanakah Formation. The McClure Mountain syenite constitutes only a small fraction of the present-day aerial exposure of the McClure Mountain igneous complex (~9.3 km²; Armbrustmacher, 1984), and the Wet Mountains and Ancestral Front Range predominantly comprise Proterozoic basement (Bickford et al., 1989). The well-rounded shape of the detrital zircon grains as observed from the backscatter images of the zircon mounts and the compositional

maturity of representative detrital zircon sandstone samples (i.e., concentration of quartz relative to other framework grains; Table 1; Fig. 4) suggest either recycling from older sedimentary strata or derivation from distal primary sources and subsequent transport over a considerable distance to the site of deposition (Leary et al., 2020).

One or more potential local secondary sources on the Colorado Plateau that could have yielded the Cambrian zircon found in the Entrada-Wanakah sedimentary interval is the Triassic basal sandstones of Chinle (New Mexico) and Dockum (Texas) strata (Dickinson and Gehrels, 2010). The Cambrian zircon deposited in the Chinle-Dockum strata, although linked to sources in the Southern Oklahoma aulacogen and Pennsylvanian Amarillo-Wichita uplift (Dickinson and Gehrels, 2008b), may have been recycled in the CCT from the exhumation of Chinle-Dockum strata by the Luning-Fencemaker thrust during Middle Jurassic time (Wyld et al., 2003; LaMaskin et al., 2011). The Devonian Temple Butte Formation sandstone in northern Arizona and southeastern Nevada is known to have minor Cambrian age signatures similar to those found in the Entrada Sandstone and Wanakah Formation, but was buried beneath thousands of meters of sedimentary strata and is thus an unlikely source (Dickinson and Gehrels, 2003).

The abundant Cambrian grains, tight clustering of concordant U-Pb ages (Fig. 5), zircon morphology, the Eu anomaly, and HREE patterns also suggest possible derivation of the Cambrian zircon grains from distal sources in the Amarillo-Wichita igneous province during the deposition of the Entrada-Wanakah interval (Fig. 10A). No other igneous assemblage in southwestern Laurentia that was uplifted during the Mesozoic is as extensive and exclusively of Cambrian age as the Amarillo-Wichita province (Dickinson and Gehrels, 2009). The sudden increase in abundance of Cambrian grains in the Entrada Sandstone "board beds", Wanakah Formation, and Tidwell Member of the Morrison Formation (aeolian, lacustrine, and fluvial deposition) allows the possibility of zircon grains having been recycled in previously deposited sediments (Lawton, 2017) that were delivered to the Cordilleran foreland by transcontinental fluvial drainages

with headwaters in southwestern Laurentia (Dickinson and Gehrels, 2009).

Provenance of Non-Cambrian Grains

The age spectra of detrital zircon deposited in Middle-Upper Jurassic strata of the Paradox Basin and CCT (Fig. 5) are similar to ages present in other Jurassic rocks of the Colorado Plateau (Fig. 10; Dickinson and Gehrels, 2008a, 2009, 2010). Sediment recycling on the Colorado Plateau was probably most prevalent during deposition of the Upper Jurassic Morrison Formation, given the overall similarity of detrital zircon age distributions in the Morrison Formation with those of the underlying older (Wanakah and Entrada) Middle Jurassic units (Fig. 5; Dickinson and Gehrels, 2008a, 2009). For example, at Ten Mile Graben, six Cambrian grains with a peak at 524 Ma constitute ~6% of the Salt Wash Member sample, suggesting possible reworking of older units (Fig. 5B). Paleocurrent data from the Upper Jurassic strata from within the Paradox Basin, CCT, and adjacent localities (Fig. 10; Peterson, 1988; Dickinson and Gehrels, 2009, 2010) show an easterly to southeasterly direction of fluvial systems, with sediments principally sourced from the south (i.e., the broad Mogollon paleohighlands that trend southeastward through central Arizona, New Mexico, and Texas) and western Cordilleran magmatic arcs (Fig. 10B). The Mogollon paleohighlands, a Late Jurassic to Early Cretaceous feature that formed contemporaneously with the Bisbee Basin in response to the rollback of the Cordilleran slab during late Mesozoic magmatism on the western margin, constituted the northern rift shoulder of the Bisbee Basin and spanned the entire southern United States-Mexico border rift belt (Fig. 10B; Dickinson and Lawton, 2001; Dickinson and Gehrels, 2008a).

In general, the non-Cambrian grains are representative of the midcontinent and southeastern Laurentia age signature in Middle–Upper Jurassic strata (Fig. 9). Other major zircon age clusters in our data set (e.g., Appalachian, 500–300 Ma; Grenvillian, 1.3–0.9 Ga; Table S1) are similar to the Mesozoic Colorado Plateau zircon distribution

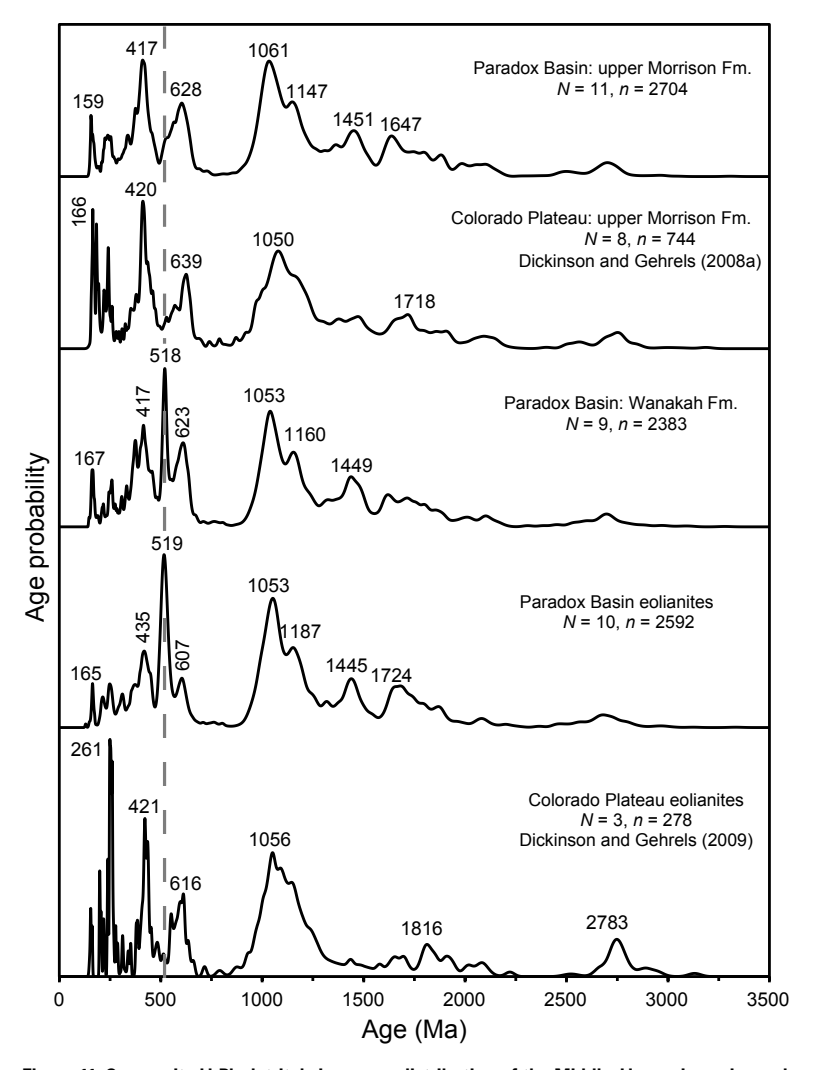


Figure 11. Composite U-Pb detrital zircon age distribution of the Middle–Upper Jurassic sandstone samples from the Paradox Basin and Central Colorado trough (this study) and the Colorado Plateau (Dickinson and Gehrels, 2008a, 2009) for comparison. Eolianite samples (Entrada Sandstone and its board beds member) and the lacustrine samples (Wanakah Formation) are Middle Jurassic, and the upper Morrison Formation samples (Tidwell and Salt Wash Members) are fluvial deposition in the Late Jurassic. *N*—number of composited samples; *n*—total number of composited grain ages; Fm.—Formation.

documented in Dickinson and Gehrels (2008a, 2009). The provenance and sediment transport history of non-Cambrian zircon grains deposited in the Middle–Upper Jurassic strata of the Paradox Basin are briefly discussed below in comparison to the regional U-Pb geochronology data set for the Colorado Plateau (Fig. 11).

Yavapai-Mazatzal (1.8–1.5 Ga) and >1.8 Ga Grains

Southwestern and northern Laurentia are underlain by Paleoproterozoic Yavapai-Mazatzal orogens (1.8-1.5 Ga) crystalline basement and early Paleoproterozoic (>1.8 Ma) to Archean (>2.5 Ga) cratons, respectively (Fig. 9). Because the Paradox Basin and CCT rest upon the underlying Yavapai-Mazatzal basement, detrital zircon from Yavapai-Mazatzal sources in the Jurassic strata of Paradox Basin imply local derivation. The younger Mazatzal detrital zircon (with age peaks between 1.7 and 1.6 Ga) are consistently more abundant than the older Yavapai (1.8-1.7 Ga) detrital grains in the Middle Jurassic units (Fig. 5), and all Yavapai-Mazatzal grains are inferred to be derived primarily from the adjacent basement core of the Ancestral Front Range (Fig. 10A). Zircon grains with ages >1.8 Ga are very limited (Fig. 5) and may have been originally sourced from a variety of sources in the Paleoproterozoic suture belt of northern Laurentia (Fig. 9). The paucity of older Paleoproterozoic and Archean grains in the sedimentary record limits any quantitative interpretation of their provenance, but their presence suggests contributions from the interior of the northern Laurentia craton delivered to the Cordilleran foreland via the intermittent Jurassic transgressions during the Mesozoic (Haq, 2018; Fig. 10).

During deposition of the Morrison Formation in Late Jurassic time, provenance shifted to the south where the Yavapai-Mazatzal basement of the Mogollon paleohighlands and Middle Jurassic aeolian strata were uplifted and stripped (Dickinson and Gehrels, 2008a), allowing primary and recycled zircon grains to be delivered to the Paradox Basin and CCT by fluvial systems (Fig. 10B).

Arc-Derived Grains (<300 Ma)

Although the Mesozoic Cordilleran magmatic arc was active on the western continental margins of Laurentia, the detrital record in the Paradox Basin and CCT (Fig. 5; Table S1) shows a nearly complete lack of zircon from the western magmatic arcs (i.e., <300 Ma grains). The low percentage of Cordilleran arc zircon in our data suggests that sediment mainly originated from orogenic sources from within and across the continent, as opposed to derivation from the proximal, contemporaneous Mesozoic Cordilleran magmatic arc along the western margin of Laurentia (Figs. 4B and 5).

Arc-derived grains with age peaks between 261 and 220 Ma are present in some of the Middle and Upper Jurassic strata but constitute a small fraction (<7%) of the entire detrital zircon distribution. The presence of arc-derived grains in the Middle Jurassic units of western Colorado and a lack in correlative units in southeastern Utah, despite the proximity to the western Cordilleran magmatic arc, suggests that the western Colorado grains may have been derived from a more southerly source in the East Mexico arc (Fig. 10A; Dickinson and Gehrels, 2003; Dickinson and Gehrels, 2009). The age peaks (261–220 Ma) of the arc-derived grains may reflect Permian-Triassic (284-232 Ma) arc accretion on the western flank of Gondwana along the Ouachita orogen following the suturing of Gondwana to Laurentia (Dickinson and Gehrels, 2010).

Minor arc-derived grains in the Upper Jurassic Tidwell and Salt Wash Members of the Morrison Formation (Fig. 5) display peaks (173-153 Ma) reflective of the contemporaneous western Cordilleran magmatic arc (Fig. 10B) and are inferred to have been delivered to the Paradox Basin via fluvial systems that originated from the Mogollon highlands. The Mogollon Highlands might have blocked contemporaneous magmatic arc grains from the western Cordillera from reaching the continental interior during deposition of the Morrison Formation. The near absence of zircon of Jurassic depositional age in the Tidwell and Salt Wash Members of the Morrison Formation in our sample suite differs slightly from age distributions (Fig. 11) previously reported by Dickinson and Gehrels (2008a), wherein 5%–17% of the detrital zircon grains are interpreted to have been derived from the Cordilleran magmatic arc.

Shift in Depositional Environments

The shift from an aeolian to a lacustrine depositional environment and coincident voluminous influx of Cambrian grains in the Entrada Sandstone and Wanakah Formation in the Paradox Basin and CCT appear to be responses to far-afield rather than local influences. We propose two major controls for the inferred sediment dispersal mechanisms and associated changes in provenance during the Middle-Late Jurassic transition: (1) the continued northward drift of the Laurentian continent during the Middle to Late Jurassic time; and (2) uplift of the Mogollon highlands. Northward drift into different wind-belt regimes significantly impacted the regional atmospheric circulation patterns over southwestern Laurentia, resulting in changing wind directions and paleoclimatic conditions (Parrish and Peterson, 1988). These climatic changes likely resulted in the intracontinental redistributive sediment transport system associated with the aeolian deposition that was pervasive on the Colorado Plateau during Middle Jurassic time (Fig. 10A). However, in Late Jurassic time, the Laurentian continent had drifted into a more temperate paleolatitude from the south, creating a wetter climate on the Colorado Plateau (May et al., 1989; Busby et al., 2005). The Morrison Formation marks the onset of this change in climate, with the deposition of lacustrine and fluvial sediments in the Paradox Basin and CCT during Late Jurassic time. We found no evidence from field observations, measured stratigraphic sections in seven transects, sandstone petrography, and U-Pb detrital zircon analyses to support the existence of the J-5 unconformity between the Morrison and Wanakah Formations in western Colorado. Data from this study support interpretations by Potter-McIntyre et al. (2016) that the Tidwell Member of the Morrison Formation and the Wanakah Formation have a conformable contact in western Colorado.

The subduction of the Farallon oceanic slab underneath the western continental margin and

the resulting arc magmatism and associated rifting on the southern margin of Laurentia created the Mogollon highlands, which significantly altered the paleodrainage, sediment provenance, and sediment dispersal routes in relation to the Paradox Basin and CCT. Paleocurrent directions in Upper Jurassic strata of the Paradox Basin show fluvial systems flowing from the southern Mogollon paleohighlands toward the east and southeast, potentially delivering sediments to the Paradox Basin and CCT during Late Jurassic time (Fig. 10B; Peterson, 1994; Dickinson and Gehrels, 2010). The Paradox Basin and CCT developed on a dynamic craton marked by active tectonic processes co-occurring at the western and eastern Laurentian margins, and the response to these processes transferred toward the continental interior.

CONCLUSIONS

We applied sediment unmixing using non-negative matrix factorization of a large detrital zircon U-Pb data set to highlight spatial and temporal patterns in sediment provenance in Middle-Upper Jurassic strata of the Paradox Basin and Central Colorado trough (CCT). Detrital zircon U-Pb age distributions suggest an interplay between extra-regional sediment supply from distant sources via transcontinental fluvial drainages (e.g., Dickinson and Gehrels, 2008a, 2009) and local sediment supply via recycling of proximal sediment in sources in central Colorado and from along the western margin of Laurentia. The most distinctive characteristic of our data is a unimodal Cambrian age peak (527-512 Ma) that is present in samples from the CCT and lacking in western Paradox Basin localities in Utah. These Cambrian grains may have been derived locally from the McClure Mountain syenite, recycled from the Chinle-Dockum strata during exhumation of the Luning-Fencemaker thrusting event during the Middle Jurassic, or sourced from the Amarillo-Wichita uplift in Oklahoma. Primary or secondary sources within the Colorado Plateau that could yield the abundant Cambrian grains in the aeolian Entrada Sandstone, lacustrine Wanakah Formation, and fluvial Tidwell Member of the Morrison Formation are limited. Given the contemporaneous paleodrainages linking the CCT to the Amarillo-Wichita uplifts, a rich Cambrian source in southwestern Laurentia during the period of deposition, we conclude the Cambrian grains were most likely sourced, at least in part, from the Amarillo-Wichita uplift in Oklahoma. The different Cambrian age peaks in modeled end members EM1 and EM3 suggest the Cambrian zircons were likely sourced from more than one igneous source. Furthermore, the size of the McClure Mountain svenite relative to a predominantly Proterozoic rocks of the Wet Mountains complex in central Colorado and the absence of a negative Eu anomaly in the McClure Mountain syenite igneous zircon, which is distinctive and present in other detrital and igneous zircons, preclude an exclusively McClure Mountain provenance for the Cambrian zircons.

Results from this study of the Middle-Upper Jurassic strata in the Paradox Basin and CCT suggest that not all the sediments were recycled from older strata, even though recycling of sediments from older strata was prevalent on the Colorado Plateau during Jurassic time. The lack of abundant Cambrian grains in the westernmost sample localities (Ten Mile Graben and Dewey Bridge) within the Paradox Basin of Utah suggests that the Uncompanded uplift acted as a barrier to sediment transport during Middle Jurassic time. Also, the lack of the distinctive Cambrian age peak in samples from the Salt Wash Member of the Morrison Formation (Upper Jurassic) suggests a cessation of sediment supply to the CCT from this distinctive source, possibly reflecting a change in sediment dispersal patterns and paleogeography during Late Jurassic time. The local tectonic framework and the nature of paleodrainage networks linking potential sediment sources vary spatially across the Western Interior sedimentary basins, providing a major control on sediment provenance.

ACKNOWLEDGMENTS

This research was funded by the American Chemical Society Petroleum Research Fund (ACS-PRF) grant 55161 (to Potter-McIntyre). The Classen Family Named Grant (an American Association of Petroleum Geologists Grants-in-Aid grant) to Ejembi benefitted this research as well. Joe Krienert and

Bolorchimeg Nanzad helped to digitize and compile some of the maps. Barry Shaulis assisted in collecting trace and rare-earth elemental data. The authors wish to thank the science editor and associate editor for editorial assistance, and Cody C. Mason and an anonymous reviewer for the constructive reviews, which significantly improved the manuscript.

REFERENCES CITED

- Armbrustmacher, T.J., 1984, Alkaline rock complexes in the Wet Mountains area, Custer and Fremont Counties, Colorado: U.S. Geological Survey Professional Paper 1269, 38 p., https://doi.org/10.3133/pp1269.
- Barbeau, D.L., 2003, A flexural model for the Paradox Basin: Implications for the tectonics of the Ancestral Rocky Mountains: Basin Research, v. 15, p. 97–115, https://doi.org/10.1046 /j.1365-2117.2003.00194.x.
- Belousova, E., Griffin, W., O'Reilly, S.Y., and Fisher, N., 2002, Igneous zircon: Trace element composition as an indicator of source rock type: Contributions to Mineralogy and Petrology, v. 143, p. 602–622, https://doi.org/10.1007/s00410 -002-0364-7.
- Bernier, J.C., and Chan, M.A., 2006, Sedimentology, depositional environments, and paleoecological context of an early Late Jurassic sauropod, Tidwell Member, Upper Jurassic Morrison Formation, east-central Utah: The Mountain Geologist, v. 43, p. 313–332.
- Bickford, M.E., Cullers, R.L., Shuster, R.D., Premo, W.R., and Van Schmus, W.R., 1989, U-Pb zircon geochronology of Proterozoic and Cambrian plutons in the Wet Mountains and southern Front Range, Colorado, in Grambling, J.A., and Tewksbury, B.J., eds., Proterozoic Geology of the Southern Rocky Mountains: Geological Society of America Special Paper 235, p. 49–64, https://doi.org/10.1130/SPE235-p49.
- Blakey, R., 2012, Paleogeography and geologic evolution of North America: On-line Accessible: http://jan.ucc.nau.edu /~rcb7/nam.html (accessed April 2018).
- Blakey, R.C., 1994, Paleogeographic and tectonic controls on some Lower and Middle Jurassic erg deposits, Colorado Plateau, in Caputo, M.V., Peterson, J.A., and Franczyk, K.J., eds., Mesozoic Systems of the Rocky Mountain Region, USA: Denver, Colorado, Rocky Mountain Section SEPM (Society for Sedimentary Geology), p. 273–298.
- Blakey, R., and Ranney, W., 2008, Ancient Landscapes of the Colorado Plateau: Grand Canyon, Arizona, Grand Canyon Association, 156 p.
- Busby, C.J., Bassett, K.N., Steiner, M.B., Riggs, N.R., Anderson, T.H., Nourse, J.A., McKee, J.W., and Steiner, M.B., 2005, Climatic and tectonic controls on Jurassic intra-arc basins related to northward drift of North America, in Anderson, T.H., Nourse, J.A., McKee, J.W., and Steiner, M.B., eds., The Mojave-Sonora Megashear Hypothesis: Development, Assessment, and Alternatives: Geological Society of America Special Paper 393, p. 359–376, https://doi.org/10.1130/0-8137-2393-0.359.
- Carr-Crabaugh, M., and Kocurek, G., 1998, Continental sequence stratigraphy of a wet eolian system: A key to relative sealevel change, in Shanley, K.W., and McCabe, P.J., eds., Relative Role of Eustasy, Climate, and Tectonism in Continental Rocks: Society for Sedimentary Geology (SEPM)

- Special Publication 59, p. 212–228, https://doi.org/10.2110/pec.98.59.0212.
- Cashion, W.B., 1973, Geologic and structure map of the Grand Junction quadrangle, Colorado and Utah: U.S. Geological Survey Miscellaneous Geologic Investigations Map I-736, scale 1:250,000, https://doi.org/10.3133/i736.
- Chapman, J.B., Gehrels, G.E., Ducea, M.N., Giesler, N., and Pullen, A., 2016, A new method for estimating parent rock trace element concentrations from zircon: Chemical Geology, v. 439, p. 59–70, https://doi.org/10.1016/j.chemgeo.2016 06 014
- Colpron, M., Crowley, J.L., Gehrels, G., Long, D.G.F., Murphy, D.C., Beranek, L., and Bickerton, L., 2015, Birth of the northern Cordilleran orogen, as recorded by detrital zircons in Jurassic synorogenic strata and regional exhumation in Yukon: Lithosphere, v. 7, p. 541–562, https://doi.org/10.1130/L451.1.
- DeCelles, P.G., 2004, Late Jurassic to Eocene evolution of the Cordilleran thrust belt and foreland basin system, western USA: American Journal of Science, v. 304, p. 105–168, https://doi.org/10.2475/ajs.304.2.105.
- Demko, T.M., Currie, B.S., and Nicoll, K.A., 2004, Regional paleoclimatic and stratigraphic implications of paleosols and fluvial/overbank architecture in the Morrison Formation (Upper Jurassic), Western Interior, USA: Sedimentary Geology, v. 167, p. 115–135, https://doi.org/10.1016/j.sedgeo .2004.01.003.
- Dickinson, W.R., and Gehrels, G.E., 2003, U-Pb ages of detrital zircons from Permian and Jurassic eolian sandstones of the Colorado Plateau, USA: Paleogeographic implications: Sedimentary Geology, v. 163, p. 29–66, https://doi.org/10 .1016/S0037-0738(03)00158-1.
- Dickinson, W.R., and Gehrels, G.E., 2008a, Sediment delivery to the Cordilleran foreland basin: Insights from U-Pb ages of detrital zircons in Upper Jurassic and Cretaceous strata of the Colorado Plateau: American Journal of Science, v. 308, p. 1041–1082.
- Dickinson, W.R., and Gehrels, G.E., 2008b, U-Pb ages of detrital zircons in relation to paleogeography: Triassic paleodrainage networks and sediment dispersal across southwest Laurentia: Journal of Sedimentary Research, v. 78, p. 745–764, https://doi.org/10.2110/jsr.2008.088.
- Dickinson, W.R., and Gehrels, G.E., 2009, U-Pb ages of detrital zircons in Jurassic eolian and associated sandstones of the Colorado Plateau: Evidence for transcontinental dispersal and intraregional recycling of sediment: Geological Society of America Bulletin, v. 121, p. 408–433, https://doi.org/10.1130/B26406.1
- Dickinson, W.R., and Gehrels, G.E., 2010, Insights into North American paleogeography and paleotectonics from U-Pb ages of detrital zircons in Mesozoic strata of the Colorado Plateau, USA: International Journal of Earth Sciences, v. 99, p. 1247–1265, https://doi.org/10.1007/s00531-009-0462-0.
- Dickinson, W.R., and Lawton, T.F., 2001, Tectonic setting and sandstone petrofacies of the Bisbee basin (USA–Mexico): Journal of South American Earth Sciences, v. 14, p. 475–504, https://doi.org/10.1016/S0895-9811(01)00046-3.
- Dickinson, W.R., and Suczek, C.A., 1979, Plate tectonics and sandstone compositions: American Association of Petroleum Geologists Bulletin, v. 63, p. 2164–2182, https://doi.org/10 .1306/2F9188FB-16CE-11D7-8645000102

- Dickinson, W.R., Gehrels, G.E., and Stern, R.J., 2010, Late Triassic Texas uplift preceding Jurassic opening of the Gulf of Mexico: Evidence from U-Pb ages of detrital zircons: Geosphere, v. 6, p. 641–662, https://doi.org/10.1130/GES00532.1.
- Fildani, A., McKay, M.P., Stockli, D., Clark, J., Dykstra, M.L., Stockli, L., and Hessler, A.M., 2016, The ancestral Mississippi drainage archived in the late Wisconsin Mississippi deep-sea fan: Geology, v. 44, p. 479–482, https://doi.org/10 .1130/G376571.
- Foster, J.R., and Lucas, S.G., eds., 2006, Paleontology and Geology of the Upper Jurassic Morrison Formation: New Mexico Museum of Natural History & Science Bulletin 36, 249 p.
- Gehrels, G., 2012, Detrital zircon U-Pb geochronology: Current methods and new opportunities, in Busby, C., and Azor, A., eds., Tectonics of Sedimentary Basins: Recent Advances: Chichester, UK, Wiley-Blackwell, p. 45–62, https://doi.org/10.1002/9781444347166.ch2.
- Gehrels, G.E., Valencia, V., and Pullen, A., 2006, Detrital zircon geochronology by Laser-Ablation Multicollector ICPMS at the Arizona LaserChron Center, in Loszewski, T., and Huff, W., eds.,. Geochronology: Emerging Opportunities, Paleontology Society Short Course: Paleontology Society Papers 12, p. 67–76, https://doi.org/10.1017/S1089332600001352.
- Gehrels, G.E., Valencia, V.A., and Ruiz, J., 2008, Enhanced precision, accuracy, efficiency, and spatial resolution of U-Pb ages by laser ablation-multicollector-inductively coupled plasma-mass spectrometry: Geochemistry Geophysics Geosystems, v. 9, p. 1–13, https://doi.org/10.1029/2007gc001805.
- Geissman, J.W., Jackson, M., Harlan, S.S., and Van Der Voo, R., 1991, Paleomagnetism of Latest Cambrian–Early Ordovician and Latest Cretaceous–Early Tertiary rocks of the Florida Mountains, southwest New Mexico: Journal of Geophysical Research, v. 96, p. 6053–6071, https://doi.org/10.1029 /90.JB02701.
- Hanson, R.E., McCleery, D.A., Crowley, J.L., Bowring, S.A., Bur-kholder, B.K., Finegan, S.A., Philips, C.M., and Pollard, J.B., 2009, Large-scale Cambrian rhyolitic volcanism in southern Oklahoma related to opening of lapetus: Geological Society of America Abstracts with Programs, v. 41, no. 2, p. 14.
- Haq, B.U., 2018, Jurassic sea-level variations: A reappraisal: GSA Today, v. 28, no. 1, p. 4–10, https://doi.org/10.1130 /GSATG359A.1.
- Hinton, R.W., and Upton, B.G.J., 1991, The chemistry of zircon: Variations within and between large crystals from syenite and alkali basalt xenoliths: Geochimica et Cosmochimica Acta, v. 55, p. 3287–3302, https://doi.org/10.1016/0016-7037 (91)90489-R.
- Hogan, J.P., and Gilbert, M.C., 1998, The Southern Oklahoma Aulacogen: A Cambrian analog for Mid-Proterozoic AMCG (Anorthosite-Mangerite-Charnockite-Granite) complexes?, in Hogan, J.P., and Gilbert, M.C., eds., Basement Tectonics 12: Central North America and Other Regions: Dordrecht, Springer, p. 39–78.
- Hoskin, P.W.O., and Ireland, T.R., 2000, Rare earth element chemistry of zircon and its use as a provenance indicator: Geology, v. 28, p. 627–630, https://doi.org/10.1130/0091-7613 (2000)28-627:REECOZ>2.0.CO;2.
- Hoskin, P.W.O., and Schaltegger, U., 2003, The composition of zircon and igneous and metamorphic petrogenesis: Reviews in Mineralogy and Geochemistry, v. 53, p. 27–62, https://doi.org/10.2113/0530027.

- Hoy, R.G., and Ridgway, K.D., 2002, Syndepositional thrust-related deformation and sedimentation in an Ancestral Rocky Mountains basin, Central Colorado trough, Colorado, USA: Geological Society of America Bulletin, v. 114, p. 804–828, https://doi.org/10.1130/0016-7606(2002)114<0804:STRDAS>2 .0.CO;2.
- Jerram, D.A., 2001, Visual comparators for degree of grain-size sorting in two and three-dimensions: Computers & Geosciences, v. 27, p. 485–492, https://doi.org/10.1016/S0098 -3004(00)00077-7.
- Kluth, C.F., and Coney, P.J., 1981, Plate tectonics of the ancestral Rocky Mountains: Geology, v. 9, p. 10–15, https://doi.org/10 .1130/0091-7613(1981)9<10:PTOTAR>2.0.CO;2.
- Kocurek, G., and Dott, R.H., Jr., 1983, Jurassic paleogeography and paleoclimate of the central and southern Rocky Mountains region, in Reynolds, M.W., and Dolly, E.D., eds., Mesozoic Paleogeography of the West-Central United States: Rocky Mountain Paleogeography Symposium 2: Denver, Colorado, Rocky Mountain Section, Society of Economic Paleontologists and Mineralogists, p. 101–116.
- LaMaskin, T.A., Vervoort, J.D., Dorsey, R.J., and Wright, J.E., 2011, Early Mesozoic paleogeography and tectonic evolution of the western United States: Insights from detrital zircon U-Pb geochronology, Blue Mountains Province, northeastern Oregon: Geological Society of America Bulletin, v. 123, p. 1939–1965, https://doi.org/10.1130/B30260.1.
- Larson, E.E., Patterson, P.E., Curtis, G., Drake, K., and Mutschler, F.E., 1985, Petrologic, paleomagnetic, and structural evidence of a Paleozoic rift system in Oklahoma, New Mexico, Colorado, and Utah: Geological Society of America Bulletin, v. 96, p. 1364–1372, https://doi.org/10.1130/0016-7606 (1985)96
- Lawton, T.F., 1994, Tectonic setting of Mesozoic sedimentary basins, Rocky Mountain region, United States, in Caputo, M.V., Peterson, J.A., and Franczyk, K.J., eds., Mesozoic Systems of the Rocky Mountain Region, USA: Denver, Colorado, Rocky Mountain Section SEPM (Society for Sedimentary Geology), p. 1–26.
- Lawton, T.F., 2017, Some other sinks and their implications for sediment routing: Geological Society of America Abstracts with Programs, v. 49, no. 6, https://doi.org/10.1130/abs /2017AM-298894.
- Leary, R.J., Umhoefer, P., Smith, M.E., Smith, T.M., Saylor, J.E., Riggs, N., Burr, G., Lodes, E., Foley, D., Licht, A., Mueller, M.A., and Baird, C., 2020, Provenance of Pennsylvanian— Permian sedimentary rocks associated with the Ancestral Rocky Mountains orogeny in southwestern Laurentia: Implications for continental-scale Laurentian sediment transport systems: Lithosphere, v. 12, p. 88–121, https://doi.org/10 .1130/L1115.1.
- Lee, D.D., and Seung, H.S., 1999, Learning the parts of objects by non-negative matrix factorization: Nature, v. 401, p. 788–791, https://doi.org/10.1038/44565.
- May, S.R., Beck, M.E., Jr., and Butler, R.F., 1989, North American apparent polar wander, plate motion, and left-oblique convergence: Late Jurassic-Early Cretaceous orogenic consequences: Tectonics, v. 8, p. 443–451, https://doi.org/10.1029/TC008i003p00443.
- McDonough, W.F., and Sun, S.-s., 1995, The composition of the Earth: Chemical Geology, v. 120, p. 223–253, https://doi.org /10.1016/0009-2541(94)00140-4.

- Nance, R.D., Murphy, J.B., and Keppie, J.D., 2002, A Cordilleran model for the evolution of Avalonia: Tectonophysics, v. 352, p. 11–31, https://doi.org/10.1016/S0040-1951(02)00187-7.
- O'Sullivan, R.B., 1980, Stratigraphic sections of Middle Jurassic San Rafael group from Wilson Arch to Bluff in southeastern Utah: U.S. Geological Survey Oil and Gas Investigations Chart OC-102, scale 422,400, https://doi.org/10.3133/oc102.
- O'Sullivan, R.B., 1992, The Jurassic Wanakah and Morrison Formations in the Telluride–Ouray–western Black Canyon area of southern Colorado: Revision of the Wanakah Formation and basal Morrison Formation in part of the Black Canyon of the Gunnison River: U.S. Geological Survey Bulletin 1927, 24 p., https://doi.org/10.3133/b1927.
- O'Sullivan, R.B., 2004, Correlation of Middle Jurassic San Rafael Group and related rocks from Bridgeport to Ouray in western Colorado: U.S. Geological Survey Scientific Investigations Map 2849, 1 sheet, https://doi.org/10.3133/sim2849.
- O'Sullivan, R.B., 2010, The lower and upper contacts of the Upper Jurassic Bluff Sandstone Member of the Morrison Formation in southeastern Utah, *in* Fassett, J.E., Zeigler, K.E., and Lueth, V.W., eds., Geology of the Four Corners Country: New Mexico Geological Society 61st Annual Fall Field Conference Guidebook, p. 101–105.
- Paces, J.B., and Miller, J.D., Jr., 1993, Precise U-Pb ages of Duluth Complex and related mafic intrusions, northeastern Minnesota: Geochronological insights to physical, petrogenetic, paleomagnetic, and tectonomagmatic processes associated with the 1.1 Ga Midcontinent Rift System: Journal of Geophysical Research, v. 98, p. 13,997–14,013, https://doi.org /10.1029/93JB01159.
- Parrish, J.T., and Peterson, F., 1988, Wind directions predicted from global circulation models and wind directions determined from eolian sandstones of the western United States—A comparison: Sedimentary Geology, v. 56, p. 261– 282, https://doi.org/10.1016/0037-0738(88)90056-5.
- Paterson, G.A., and Heslop, D., 2015, New methods for unmixing sediment grain size data: Geochemistry Geophysics Geosystems, v. 16, p. 4494–4506, https://doi.org/10.1002 /2015GC006070.
- Pearce, N.J., Perkins, W.T., Westgate, J.A., Gorton, M.P., Jackson, S.E., Neal, C.R., and Chenery, S.P., 1997, A compilation of new and published major and trace element data for NIST SRM 610 and NIST SRM 612 glass reference materials: Geostandards Newsletter, v. 21, p. 115–144, https://doi.org/10.1111/j.1751-908X.1997.tb00538.x.
- Pell, S.D., Williams, I.S., and Chivas, A.R., 1997, The use of protolith zircon-age fingerprints in determining the protosource areas for some Australian dune sands: Sedimentary Geology, v. 109, p. 233–260, https://doi.org/10.1016/S0037-0738 (96)00061-9.
- Peterson, F., 1988, Pennsylvanian to Jurassic eolian transportation systems in the western United States: Sedimentary Geology, v. 56, p. 207–260, https://doi.org/10.1016/0037-0738 (88)90055-3.
- Peterson, F., 1994, Sand dunes, sabkhas, streams, and shallow seas: Jurassic paleogeography in the southern part of the Western Interior Basin, *in* Caputo, M.V., Peterson, J.A., and Franczyk, K.J., eds., Mesozoic Systems of the

- Rocky Mountain Region, USA: Denver, Colorado, Rocky Mountain Section SEPM (Society for Sedimentary Geology), p. 233–272.
- Pipiringos, G.N., and O'Sullivan, R.B., 1978, Principal unconformities in Triassic and Jurassic rocks, Western Interior United States: A preliminary survey: U.S. Geological Survey Professional Paper 1035-A, 29 p., https://doi.org/10.3133/pp1035A.
- Pivarunas, A.F., and Meert, J.G., 2019, Protracted magmatism and magnetization around the McClure Mountain alkaline igneous complex: Lithosphere, v. 11, p. 590–602, https://doi .org/10.1130/L1062.1.
- Potter-McIntyre, S.L., Boraas, M., DePriest, K., and Aslan, A., 2016, Middle Jurassic landscape evolution of southwest Laurentia using detrital zircon geochronology: Lithosphere, v. 8, p. 185–193, https://doi.org/10.1130/L467.1.
- Powell, B.N., Gilbert, M.C., and Fischer, J.F., 1980, Lithostratigraphic classification of basement rocks of the Wichita province, Oklahoma: Summary: Geological Society of America Bulletin, v. 91, p. 509–514, https://doi.org/10.1130/0016 -7606(1980)91<509:LCOBRO>2.0.CO;2.
- Powers, M.C., 1953, A new roundness scale for sedimentary particles: Journal of Sedimentary Petrology, v. 23, p. 117–119, https:// doi.org/10.1306/D4269567-2B26-11D7-8648000102C1865D.
- Rahl, J.M., Reiners, P.W., Campbell, I.H., Nicolescu, S., and Allen, C.M., 2003, Combined single-grain (U-Th)/He and U/Pb dating of detrital zircons from the Navajo Sandstone, Utah: Geology, v. 31, p. 761–764, https://doi.org/10.1130/G19653.1
- Rubatto, D., 2002, Zircon trace element geochemistry: Partitioning with garnet and the link between U-Pb ages and metamorphism: Chemical Geology, v. 184, p. 123–138, https://doi.org/10.1016/S0009-2541(01)00355-2.
- Saylor, J.E., Sundell, K.E., and Sharman, G.R., 2019, Characterizing sediment sources by non-negative matrix factorization of detrital geochronological data: Earth and Planetary Science Letters, v. 512, p. 46–58, https://doi.org/10.1016/j.epsl.2019.01.044.
- Schaltegger, U., Fanning, C.M., Günther, D., Maurin, J.C., Schulmann, K., and Gebauer, D., 1999, Growth, annealing and recrystallization of zircon and preservation of monazite in high-grade metamorphism: Conventional and in-situ U-Pb isotope, cathodoluminescence and microchemical evidence: Contributions to Mineralogy and Petrology, v. 134, p. 186–201, https://doi.org/10.1007/s004100050478.
- Schoene, B., and Bowring, S.A., 2006, U-Pb systematics of the McClure Mountain syenite: Thermochronological constraints on the age of the ⁴⁰Ar/⁵⁹Ar standard MMhb: Contributions to Mineralogy and Petrology, v. 151, p. 615–630, https://doi.org/10.1007/s00410-006-0077-4.
- Schwartz, T.M., Schwartz, R.K., and Weislogel, A.L., 2019, Orogenic recycling of detrital zircons characterizes age distributions of North American Cordilleran strata: Tectonics, v. 38, p. 4320–4334, https://doi.org/10.1029/2019TC005810.
- Scott, R.B., Harding, A.E., Hood, W.C., Cole, R.D., Livaccari, R.F., Johnson, J.B., Shroba, R.R., and Dickerson, R.P., 2001, Geologic map of Colorado National Monument and adjacent areas, Mesa County, Colorado: U.S. Geological Survey Geologic Investigations Series I-2740, scale 24,000, with 40 p. text, https://doi.org/10.3133/2740.

- Sharman, G.R., and Johnstone, S.A., 2017, Sediment unmixing using detrital geochronology: Earth and Planetary Science Letters, v. 477, p. 183–194, https://doi.org/10.1016/j.epsl.2017 .07044.
- Sharman, G.R., Sharman, J.P., and Sylvester, Z., 2018a, detritalPy: A Python-based toolset for visualizing and analysing detrital geo-thermochronologic data: The Depositional Record, v. 4, p. 202–215, https://doi.org/10.1002/dep2.45.
- Sharman, G.R., Stockli, D.F., Flaig, P.P., Raynolds, R.G., and Covault, J.A., 2018b, Local-to-distant provenance cyclicity of the southern Front Range, central Colorado: Insights from detrital zircon geochronology, in Ingersoll, R.V., Lawton, T.F., and Graham, S.A., eds., Tectonics, Sedimentary Basins, and Provenance: A Celebration of William R. Dickinson's Career: Geological Society of America Special Paper 540, p. 547–569, https://doi.org/10.1130/2018.2540(24).
- Sláma, J., Košler, J., Condon, D.J., Crowley, J.L., Gerdes, A., Hanchar, J.M., Horstwood, M.S.A., Morris, G.A., Nasdala, L., Norberg, N., Schaltegger, U., Schoene, B., Tubrett, M.N., and Whitehouse, M.J., 2008, Plešovice zircon—A new natural reference material for U-Pb and Hf isotopic microanalysis: Chemical Geology, v. 249, p. 1–35, https://doi.org/10.1016/j .chemgeo.2007.11.005.
- Steven, T.A., Lipman, P.W., Hail, W.J., Jr., Barker, F., and Luedke, R.G., 1974, Geologic map of the Durango quadrangle, southwestern Colorado: U.S. Geological Survey Miscellaneous Investigations Map I-764, scale 1:250,000, https://doi.org /10.3133/i764.
- Tanner, W.F., 1970, Triassic-Jurassic lakes in New Mexico: The Mountain Geologist, v. 7, p. 281–289.
- Thomas, W.A., 2011, Detrital-zircon geochronology and sedimentary provenance: Lithosphere, v. 3, p. 304–308, https:// doi.org/10.1130/RFL001.1.
- Tweto, O., Steven, T.A., Hail, W.J., Jr., and Moench, R.H., 1976, Preliminary geologic map of the Montrose 1° × 2° quadrangle, southwestern Colorado: U.S. Geological Survey Miscellaneous Field Studies Map MF-761, scale 1:250,000, https://doi.org/10.3133/mf761.
- Tweto, O., Moench, R.H., and Reed, J.C., Jr., 1978, Geologic map of the Leadville 1°× 2° quadrangle, northwestern Colorado: U.S. Geological Survey Miscellaneous Investigations Series Map I-999, scale 1:250,000, https://doi.org/10.3133/i999.
- Weltje, G.J., 1997, End-member modeling of compositional data: Numerical-statistical algorithms for solving the explicit mixing problem: Mathematical Geology, v. 29, p. 503–549, https://doi.org/10.1007/BF02775085.
- Weltje, G.J., and Prins, M.A., 2003, Muddled or mixed? Inferring palaeoclimate from size distributions of deep-sea clastics: Sedimentary Geology, v. 162, p. 39–62, https://doi.org/10 .1016/S0037-0738(03)00235-5.
- Whitmeyer, S.J., and Karlstrom, K.E., 2007, Tectonic model for the Proterozoic growth of North America: Geosphere, v. 3, p. 220–259, https://doi.org/10.1130/GES00055.1.
- Wyld, S.J., Rogers, J.W., and Copeland, P., 2003, Metamorphic evolution of the Luning-Fencemaker fold-thrust belt, Nevada: Illite crystallinity, metamorphic petrology, and 40 Ar/s⁹⁸ Ar geochronology: The Journal of Geology, v. 111, p. 17–38, https://doi.org/10.1086/344663.